

University of Massachusetts Medical School
eScholarship@UMMS

GSBS Dissertations and Theses

Graduate School of Biomedical Sciences

2011-05-24

The Importance of the Centrosomal Localization Sequence of Cyclin E for Promoting Centrosome Duplication: A Dissertation

Joshua J. Nordberg
University of Massachusetts Medical School

Let us know how access to this document benefits you.

Follow this and additional works at: https://escholarship.umassmed.edu/gsbs_diss

 Part of the [Cell Biology Commons](#), [Cells Commons](#), and the [Enzymes and Coenzymes Commons](#)

Repository Citation

Nordberg JJ. (2011). The Importance of the Centrosomal Localization Sequence of Cyclin E for Promoting Centrosome Duplication: A Dissertation. GSBS Dissertations and Theses. <https://doi.org/10.13028/et69-4039>. Retrieved from https://escholarship.umassmed.edu/gsbs_diss/547

This material is brought to you by eScholarship@UMMS. It has been accepted for inclusion in GSBS Dissertations and Theses by an authorized administrator of eScholarship@UMMS. For more information, please contact Lisa.Palmer@umassmed.edu.

THE IMPORTANCE OF THE CENTROSOMAL LOCALIZATION SEQUENCE OF
CYCLIN E FOR PROMOTING CENTROSOME DUPLICATION

A Dissertation Presented

By

JOSHUA JOHN NORDBERG

Submitted to the Faculty of the
University of Massachusetts Graduate School of Biomedical Sciences, Worcester
In partial fulfillment of the requirements for the degree of

DOCTOR OF PHILOSOPHY

MAY 24, 2011

CELL BIOLOGY

THE IMPORTANCE OF THE CENTROSOMAL LOCALIZATION SEQUENCE OF
CYCLIN E FOR PROMOTING CENTROSOME DUPLICATION

A Dissertation Presented

By

JOSHUA JOHN NORDBERG

The signatures of the Dissertation Defense Committee signifies completion and approval as to style and content of the Dissertation

Greenfield Sluder, Ph.D., Thesis Advisor

Kirsten Hagstrom Ph.D., Member of Committee

Edward Hinchcliffe Ph.D., Member of Committee

Stephen Jones Ph.D., Member of Committee

William Theurkauf Ph.D., Member of Committee

The signature of the Chair of the Committee signifies that the written dissertation meets the requirements of the Dissertation Committee

Dannel McCollum Ph.D., Chair of Committee

The signature of the Dean of the Graduate School of Biomedical Sciences signifies that the student has met all graduation requirements of the school.

Anthony Carruthers, Ph.D., Dean of the Graduate School of Biomedical Sciences

Interdisciplinary Graduate Program

May 24, 2011

I dedicate this work to my loving and supportive wife, Lauren Copp Nordberg,
without whom I could not have found the strength and commitment
to complete this endeavor.

Thank you.

Acknowledgements

It could be said that nothing great comes without great sacrifice. Nothing could be truer regarding the completion of this Ph.D. program. However, the experiences I have had and the knowledge I have gained were worth every bit of pain they caused. Some of the pain and most of the knowledge gained can be attributed to my advisor and mentor, Dr. Greenfield (Kip) Sluder. I had the pleasure of working under Kip's tutelage for 10 years. In that time I learned to never fear a piece of equipment, to always look at the big picture, and above all else, to enjoy working in the lab. Kip has an unmatched sense of biological significance, and an uncanny ability to make the impossible seem worthy of the challenge. There was never an experiment too crazy to try.

I would like to extend my thanks also to my advisory committee: Drs. Dannel McCollum, William Theurkauf, Kirsten Hagstrom and Stephen Jones. Thank you for your guidance over the years and your help in shaping my project appropriately to keep me on track. I also thank Dr. Edward (Ted) Hinchcliffe for helpful discussions and comments and for serving as an outside member of my committee.

I would also like to take this opportunity to extend my most sincere thanks to the people who work on the third floor of the Biotech Four building. The researchers, the students, and the support staff have been colleagues of unparalleled excellence. James Carey became a great friend as well as a frequent teacher of molecular biology. Beth Luna was a veritable fountain of

knowledge of all things biochemical. In addition to the community of researchers, Denise Maclachlan, Cathy Warren and Donna Castellanos have made immeasurable contributions to this work through their kindness and support on all manner of day-to-day matters.

All the members of the Sluder Lab, past and present, also left their indelible mark on my scientific career. Rick Miller and Ted Hinchcliffe were the first people I met in the lab, and they gave me the foundation for everything I know about microscopy. Anna Krzywicka-Racka and Yumi Uetake have been wonderful mentors as senior post-docs in the lab. Christopher English allowed me to practice my teaching on him, and he seemed to like it. And although Stephen Douthwright and Toshi Hatano were recent additions to the lab, and as such I did not get to know them as well as I would have liked, they were a pleasure to work with as I was completing my research.

And last but not least, I would like to formally thank my family. My wife Lauren, our son Elliot, and our daughter Claire all provided me with a wonderful reason to go home from lab every night. My dad has always been an excellent listener when things weren't going the way I wanted them to. And finally, my mother has been an amazing source of encouragement and support throughout my entire time in graduate school...and life.

My deepest and most sincere thanks to you all.

Abstract

This thesis comprises three separate studies that investigate the consequences of supernumary centrosomes, the effect of centrosome loss, and a control mechanism for regulating CDK2/cyclin E activity in centrosome duplication.

The centrosome is the major microtubule-organizing center of the cell. When the cell enters mitosis, it is of critical importance that the cell has exactly two centrosomes in order to properly segregate the chromosomes to two daughter cells. Supernumary centrosomes are a problem for the cell in that they increase the incidence of chromosomal instability. Aberrant centrosome numbers are seen in a number of cancers, and there has been a proposed connection between the loss of function of p53 and multiple centrosomes. We investigated the consequences of multiple centrosomes in p53-null mouse embryonic fibroblasts (MEFs) to determine how cells with multiple centrosomes can continue to propagate and become cancer. We found that even in the face of extra centrosomes, p53-null MEFs are able to divide in a bipolar fashion by bundling extra centrosomes into two spindle poles.

The centrosome has also been proposed to play a role in cell cycle control. We followed up on a previous study, which had suggested that centrosome loss causes a G1 arrest. We found that cells did not arrest in G1 due to centrosome removal as previously reported, but instead the arrest was

dependent on additional stressors, namely the incident light used for our long-term live-cell observations. Our study showed that centrosome loss is a detectable stress that, in conjunction with additional stresses, can contribute to cell cycle arrest.

It is known that CDK2/cyclin E activity is required to promote centrosome duplication. But with the discovery of a centrosomal localization sequence (CLS) in cyclin E, we wanted to know if centrosome duplication required a specific sub-cellular localization of CDK2 kinase activity. We found that centrosome duplication in *Xenopus* extract was dependent on CLS-mediated centrosomal localization of cyclin E, in complex with CDK2. Our results point to a mechanism for regulating centrosome duplication in the face of high cytoplasmic CDK2/cyclin E kinase activity.

Table of Contents

Approval Page	iii
Dedication	iv
Acknowledgements	v
Abstract	vii
Table of Contents	ix
List of Tables	xi
List of Figures	xii
List of Abbreviations	xiv
Preface	xv
Chapter I:	1
General Introduction	
Chapter II:	14
Practical Aspects of Adjusting Digital Cameras	
Introduction	15
Measuring Gray-Level Information	15
Camera Settings	19
Contrast Stretching	24
Camera Versus Image Display Controls	31
Chapter III:	33
The Good, The Bad, and The Ugly: Practical Consequences of Centrosome Amplification	
Abstract	34
Introduction	35
Results/Discussion	37
Conclusions	48
Materials and Methods	50
Chapter IV:	52
The Importance of the Centrosomal Localization Sequence of Cyclin E for Promoting Centrosome Duplication in <i>Xenopus</i> Extract	
Abstract	53
Introduction	54
Results	57
Discussion	74
Future Directions	80
Materials and Methods	86

Chapter V: General Discussion	93
Appendix A: Centrosome loss is a stress that, when combined with other stresses, causes cell cycle arrest.	104
Abstract	105
Introduction	106
Results	108
Discussion	113
Materials and Methods	115
Appendix B: Detailed Protocol for Observing Centrosome Duplication In a Cell-Free Extract Made From <i>Xenopus laevis</i> Oocytes	117
Making of <i>Xenopus</i> Egg Extract	118
Quantitation of Centrosome Duplication in <i>Xenopus</i> extracts	123
References	125

List of Tables**CHAPTER IV Tables**

Table 4.1	Comparison of average number of centrosome doublings in a 6-hour period	66
Table 4.2	Comparison of Average Centrosome Duplication Times	70

List of Figures

Chapter I Figures

Figure 1.1	Structure of the Centrosome	3
Figure 1.2	Schematic Representation of the Centrosome Cycle	7

Chapter II Figures

Figure 2.1	Two ways to measure pixel gray values	17
Figure 2.2	Adjusting camera offset	21
Figure 2.3	Adjusting camera gain	23
Figure 2.4	Optimizing image contrast using the line scan plot	26
Figure 2.5	Optimizing the image using the histogram	28-29
Figure 2.6	The importance of scaling the y-axis of the histogram under some circumstances	30

Chapter III Figures

Figure 3.1	Range of spindle morphologies in p53 ^{-/-} mouse embryo fibroblasts	41
Figure 3.2	Comparison of mitotic outcomes in p53 ^{-/-} MEF and NIH3T3 cells	44
Figure 3.3	Mitosis in two adjacent binucleate BSC-1 cells, each containing four centrosomes	46

Chapter IV Figures

Figure 4.1	Quantifying centrosome duplication using Polarization Microscopy	58
Figure 4.2	Protein expression from mRNA in <i>Xenopus</i> extract	60
Figure 4.3	Percentage of centrosomes that duplicate at each round	63

Figure 4.4	Average number of centrosome duplications per 6-hour period	65
Figure 4.5	The timing of centrosome duplication events	69
Figure 4.6	Localization of GFP-cyclin E in <i>Xenopus</i> extracts	72
Figure 4.7	Localization of GFP-cyclin E in <i>Xenopus</i> S3 cells	73

Appendix A Figures

Figure A.1	Cell manipulation and viewing chambers	109
Figure A.2	Cell Cycle Progression of BSC-1 Karyoplasts	111
Figure A.3	G1 progression of acentrosomal and control cut BSC-1 cells under various experimental conditions	112

List of Abbreviations

DIC: Differential Interference Contrast

CDK2: Cyclin Dependent Kinase 2

CLS: Centrosome Localization Sequence

R128A: Mutant form of cyclin E that does not bind CDK2

SW/RA: Mutant form of cyclin E that does not bind CDK2 or centrosome

MEF: Mouse Embryonic Fibroblast

BSC-1: African green monkey kidney epithelial cells

hTERT-RPE-1: Human telomerase-immortalized Retinal Pigment Epithelial cell

BrdU: 5-bromo-2'deoxyuridine

Preface

Portions of this dissertation are contained in the following publications:

Uetake Y, Loncarek J, **Nordberg JJ**, English CN, La Terra S, Khodjakov A, Sluder G. Cell cycle progression and de novo centriole assembly after centrosomal removal in untransformed human cells. *The Journal of Cell Biology* (2007) vol. 176 (2) pp. 173-82

Nordberg JJ and Sluder G. Practical aspects of adjusting digital cameras. *Methods in Cell Biology* (2007) vol. 81 pp. 159-69

Sluder G and **Nordberg JJ**. The good, the bad and the ugly: the practical consequences of centrosome amplification. *Current Opinion in Cell Biology* (2004) vol. 16 (1) pp. 49-54

Figure 1.1 was reprinted with permission from Nature Publishing Group: License # 2663871063795

Figure 1.2 was reprinted with permission pending from Wiley-VCH:

Figure A.3 was made in collaboration with Yumi Uetake.

Chapter I

General Introduction

Centrosome Structure

The centrosome acts as the microtubule-organizing center of a cell (MTOC). During interphase it acts to nucleate the growth of new microtubules as well as organize them. It can direct the direction of migration in neuronal cells by orienting the microtubule array to the leading edge of the cell (Solecki et al., 2004) and it helps determine polarity of differentiated cells (Meads and Schroer, 1995) (reviewed in: Musch, 2004). In some cell types, the mother centriole becomes the basal body for a primary cilium (Rieder et al., 2001).

The central components of the interphase centrosome are two barrel-shaped, microtubule-based structures called centrioles. The microtubules that make up the centrioles are highly modified in higher eukaryotes. Instead of a single microtubule, the walls of the centriole are composed of triplet microtubules in which the main tubule (the A-tubule) is the only complete tubule while the B tubule shares its wall with A and the C-tubule shares its wall with B. There are nine of these triplet blades arranged into a barrel creating a pinwheel-like shape. This ultrastructure can be seen in the electron micrograph in Figure 1.1.a and in diagrammatic form in Figure 1.1.b.

Surrounding the centrioles is a 'cloud' of centrosome-associated proteins known collectively as the peri-centriolar material (PCM) (Schnackenberg and Palazzo, 1999), (Figure 1.1.a, arrowheads). One prominent PCM protein is the gamma isoform of tubulin (γ -tubulin), which is a key component of

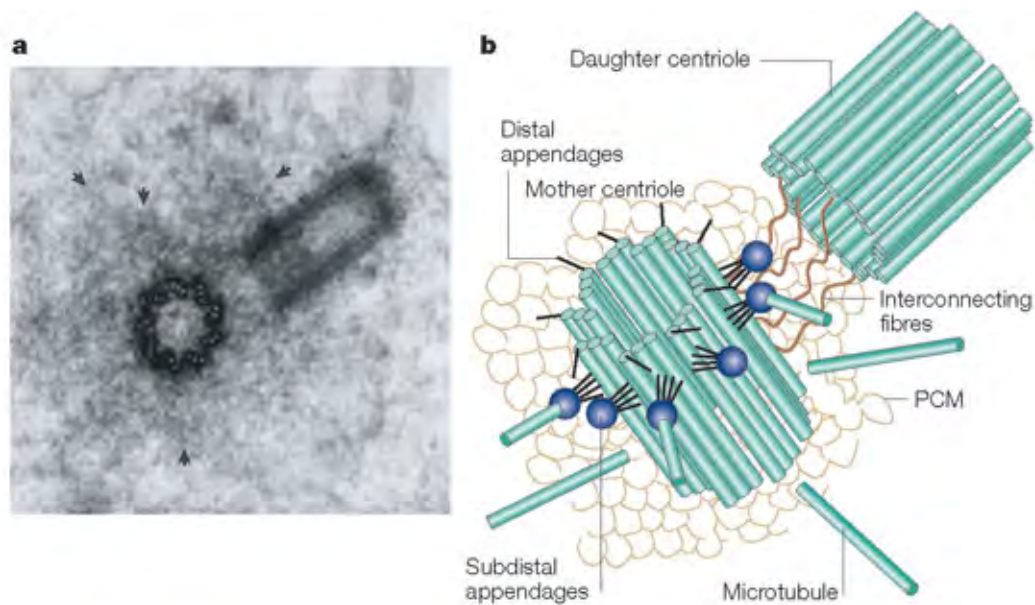


Figure 1.1 – Structure of the Centrosome. The centrosome consists of two microtubule-based structures, the centrioles, surrounded by a matrix of pericentrosomal material (PCM). An electron micrograph (a) shows a pair of orthogonally oriented centrioles. On the left is a cross-section of one centriole showing the pinwheel arrangement of triplet microtubule blades. On the right is a sagittal section through the other centriole. The arrowheads indicate the outer reaches of the PCM. A diagrammatic representation of the centrosome (b) shows additional structures. The older or “mother” centriole is recognized by the presence of distal and sub-distal appendages at the end of the microtubule barrel. The newer “daughter” centriole is closely associated with the mother and lacks appendages. Microtubules are seen emanating from the PCM. The centrioles don’t play a direct role in nucleation of microtubules, but γ -tubulin ring complexes (γ -TuRCs) are known to be concentrated in the PCM, which confers the microtubule-nucleation function to the centrosome. Part **a** of the figure is reproduced with permission from (Rieder and Borisy, 1982). Part **b** is modified with permission from (Doxsey, 2001a).

the γ -tubulin Ring Complexes (γ -TURCs) known to be required for the nucleation of new microtubules. Recent studies have shown that the amount of PCM also directly correlates with the potential of a single mother centriole to form multiple daughter centrioles in some cell lines (Loncarek et al., 2008).

During interphase, the centrosome has been proposed to act as a site of catalytic activity (Rieder et al., 2001; Doxsey, 2001b). The centrosome accumulates many different proteins and protein complexes (Delaval and Doxsey, 2010). Some proteins, for example cyclin E, are transported to the centrosome in a directed fashion (Matsumoto and Maller, 2004). Other proteins may end up at the centrosome simply because it is the center of the cell's microtubule network and thus a natural terminus of minus-end directed microtubule motor proteins. Regardless of the particular mechanism, the concentration of various enzymes to the centrosome seems to play an important role in controlling cell cycle progression (Rieder et al., 2001; Hinchcliffe et al., 2001; Mikule et al., 2007) and promoting DNA duplication (Matsumoto and Maller, 2004; Ferguson and Maller, 2010).

Centrosomes in Mitosis

The cell should have two centrosomes upon entry into mitosis. During mitosis, the centrosomes act in a dominant fashion to determine the polarity of the mitotic spindle apparatus (Heald et al., 1997). Microtubules that emanate from the spindle poles attach to the kinetochores of chromosomes (Rieder and

Salmon, 1998) and provide the tracks on which the chromosomes will segregate to daughter cells. In addition to the chromosome-associated microtubules, the centrosomes also nucleate and organize astral microtubules that interact with the cell cortex. This cortical interaction plays a critical role in positioning the spindle along the appropriate axis to allow for efficient cytokinesis (Rieder et al., 2001). Ultimately the number of centrosomes present in the cell during mitosis will have a profound impact on the success or failure of mitosis.

Cells without centrosomes can still form a proper bipolar mitotic spindle in some cases. In fact, cells made acentrosomal by microsurgery form a bipolar spindle 61% of the time (Hornick et al., 2011). This does not mean the centrosomes are dispensable for normal mitosis. Acentrosomal spindle poles lack the astral microtubules necessary for the cortical interaction and proper spindle positioning and thus have an increased rate of cytokinesis failure due to spindle positioning defects (Khodjakov and Rieder, 2001). In addition, localization of the centrosome to the site of the spindle mid-body was shown to be required for proper abscission and completion of cytokinesis (Piel et al., 2001).

Centrosome Duplication

During G1, the cell possesses a single centrosome consisting of a pair of centrioles surrounded by a cloud of PCM. The centrosome must duplicate once and only once per cell cycle. Under normal circumstances, particularly in higher eukaryotes, the centrosome is duplicated simultaneously with the DNA with both

processes initiated by the rise in CDK2-cyclin E kinase activity (Matsumoto et al., 1999; Hinchcliffe et al., 1999; Lacey et al., 1999; van and Harlow, 1993; Rosenblatt et al., 1992).

Figure 1.2 provides an overview of the centrosome duplication cycle. Centrosome duplication could be considered to begin at the very end of the previous mitosis as the cell is re-entering G1. By this time the two centrioles have been disoriented from one another, presumably by the action of the anaphase-promoting enzyme, separase (Tsou and Stearns, 2006). As the cell enters S phase, small pro-centrioles begin to form adjacent to the existing centrioles. The pro-centrioles continue to elongate during S-phase becoming *bona fide* daughter centrioles. Throughout the remaining time in S-phase there is a mechanism in place to prevent another round of duplication. This block is regulated, in part, by the presence of the newly formed daughter centriole. The two centrosomes then begin a process of maturation throughout G2. During this time the centrosomes accumulate additional PCM, move away from one another, and position themselves to become the mitotic spindle poles (reviewed in Sluder, 2004).

How centrosome duplication is rigorously controlled has not been fully described. Many advances have been made to augment our understanding of how new centrosomes are formed. The generally accepted process is that

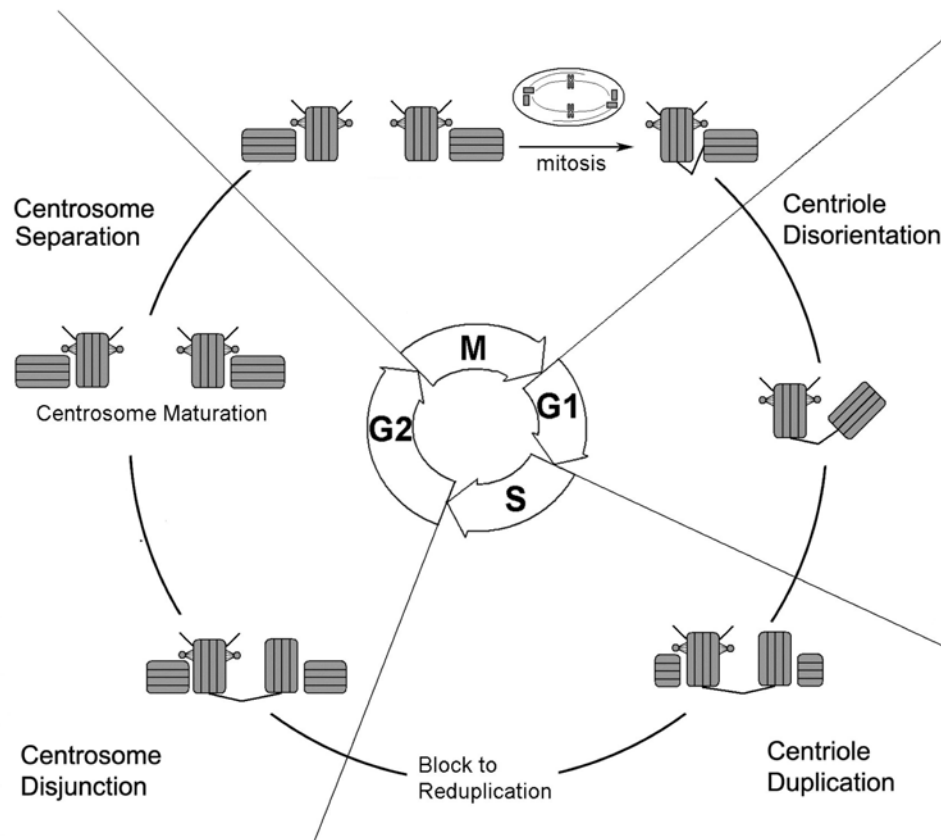


Figure 1.2 – Schematic Representation of the Centrosome Cycle. The centrioles are shown as small shaded barrels. The four phases of the cell cycle are shown in the middle, advancing in a clockwise direction from the top-right. The G1 cell has inherited a single centrosome from the preceding mitosis. The process of disorientation has already begun as the close association of the mother and daughter centrioles has been relieved by the action of separase (Tsou and Stearns, 2006). In S-phase, pro-centrioles begin to form adjacent at right angles to the proximal ends of the existing centrioles, eventually becoming daughter centrioles. The block to reduplication is believed to be due to the close physical association of mother and newly formed daughter centrioles (Tsou and Stearns, 2006; Loncarek et al., 2008a). In G2, the centrosomes disjoin from one another and the centrosomes mature. This can be observed by the appearance of the distal and subdistal appendages on the former daughter centriole from the previous cell cycle. The two centrosomes eventually become the spindle poles in mitosis and each is partitioned to the two daughter cells. Figure reprinted with permission from (Sluder, 2004)

activation of Plk4 begins a cascade of steps recruiting the necessary materials for building centrioles (Dammerman et al., 2008; Rodrigues-Martins et al., 2007; Kleylein-Sohn et al., 2007). SAS-6 is the first protein recruited to the site and is a key structural element for new centriole formation. New daughter centrioles are then assembled adjacent to the existing centrioles by the addition of tubulin subunits under a CP110 “cap.” The centrioles are finally stabilized by polyglutamylation of the tubulin subunits (Kleylein-Sohn et al., 2007).

Centrosomes and the Cell Cycle

Although advancing through the cell cycle from G1 to S is the trigger for promoting centrosome duplication, the centrosomes are not merely followers of the cell cycle. As mentioned above, the centrosome is thought to provide a site for concentrating proteins and catalyzing enzymatic reactions (Rieder et al., 2001). The idea of the centrosome as a catalytic center is supported by observations that the centrosome is important for controlling cell cycle progression.

Microsurgical removal of the centrosome does not affect the cell cycle during which the centrosome was removed, however it activates a cell cycle arrest in the subsequent mitosis (Hinchcliffe et al., 2001). This arrest is not triggered solely by the loss of the centrosome, but is in fact a p38-dependent stress response that arrests the cell in G1 (Uetake et al., 2007). RNAi of centrosomal proteins also causes a p53-mediated G1 arrest in human cells

(Mikule et al., 2007). Taken together, these observations present an interesting new paradigm in which the centrosome must be present and healthy in order to promote cell cycle progression.

Cells that escape arrest in G1 of the subsequent cell cycle, i.e. those that do not surpass the threshold for the stress response, are able to re-form centrioles *de novo* as the cell enters S-phase (Uetake et al., 2007). This phenomenon was not peculiar to transformed cells as this was observed in two non-transformed human cell lines. The reformation of centrioles before mitosis is an interesting observation that highlights their importance to the cell.

Centrosomes and Cancer

Having two centrosomes at the time of mitosis is crucial to maintaining mitotic fidelity. Theodor Boveri first proposed a connection between centrosome number and cancer in 1914 (Boveri, 1914). Since that time, many studies have shown that cells of a variety of later-stage cancers tend to have supernumerary centrosomes (Lingle et al., 1998; Lingle and Salisbury, 1999; Lingle and Salisbury, 2000; Lingle et al., 2002; D'assoro et al., 2002; Pihan et al., 1998; Pihan et al., 2001; Pihan et al., 2003). There have also been studies that demonstrate connections between mutations in several known oncogenes and deregulation of centrosome duplication (Fukasawa et al., 1996; Chiba et al., 2000; Tarapore and Fukasawa, 2002), reviewed in (Fukasawa, 2007; Nigg, 2002).

If the centrosome fails to duplicate, the cell will only have one centrosome at mitosis and may build a monopolar spindle, or a bipolar spindle with one pole lacking a centrosome (O'Connell et al., 2001). In a cell with a monopolar spindle, the chromosomes will not be segregated to two daughters, and the cell will exit mitosis in a tetraploid state. Tetraploidy has been a proposed intermediate step on the road to aneuploidy, a characteristic shared by many cancers (Levine et al., 1991; Galipeau et al., 1996; Shackney et al., 1989; Southern et al., 1997; Shi and King, 2005).

A more direct road to aneuploidy is the result of a cell entering mitosis with more than two centrosomes. In the presence of extra centrosomes, there is the possibility of chromosome segregation to more than two daughter cells. A multipolar cell division would absolutely lead to whole chromosome gains or losses. The effect of extra centrosomes is not always so extreme, however. In many cases, mitotic cells with multiple centrosomes are able to undergo a bipolar cleavage due to spindle pole bundling (Sluder and Nordberg, 2004; Levesque et al., 2003; Quintyne et al., 2005), but chromosomal instability is still elevated in these multipolar cells (Ganem et al., 2009). The chromosome segregation errors are believed to be due to lagging chromosomes that result from merotelic attachment of chromosomes to microtubules during the time when the extra spindle poles are being coalesced (Ganem et al., 2009).

Controlling Centrosome Duplication

The fact that centrosome number so heavily influences the polarity of the mitotic spindle, the fidelity of chromosome distribution, and the success of cytokinesis, points to the importance of maintaining correct centrosome number. Since the cell does not have an intrinsic checkpoint to monitor centrosome number before the cell enters mitosis, it is critical for the cell to tightly regulate the duplication process (Sluder et al., 1997). Centrosome duplication is known to be coordinated with DNA duplication. Both are initiated during, and limited to, S-phase; and both processes are initiated by the rise of CDK2/cyclin E activity (Hinchcliffe et al., 1999; Lacey et al., 1999) reviewed in (Hinchcliffe and Sluder, 2002).

The current thinking is that cells possess a centrosome-intrinsic block to reduplication (Tsou and Stearns, 2006; Wong and Stearns, 2003). The close physical association of the newly formed daughter centriole with the mother is believed to prevent further doubling. At the end of mitosis, this tight association is relieved by the activation of the anaphase-promoting enzyme, separase which leads to the visible separation of mother and daughter centrioles seen in G1 phase (Tsou and Stearns, 2006). The proximity-based block has been tested by laser-ablation of newly formed daughter centrioles in an attempt to relieve the block to duplication. In S-phase arrested HeLa cells, mother centrioles develop new daughter centrioles within about 4 hours of ablation (Loncarek et al., 2008).

Overexpression of Plk4 (Kleylein-Sohn et al., 2007), pericentrin (Loncarek et al., 2008a), or SAS-6 (Rodrigues-Martins et al., 2007) has each been shown to

increase the number of daughter centrioles that form around a mother during duplication. So, even though the presence of a daughter centriole adjacent to a mother provides a block to reduplication, a clear question remains. How does the cell control the number of daughters that form around the mother in the first place, when it is clear that the mother centriole has the capacity to form daughters at multiple sites? It seems that controlling the levels of these upstream effectors would be critical to the fidelity of the centrosome duplication process.

The Centrosome Localization Sequence

Recent work from the lab of James Maller has revealed a conserved 20 amino-acid sequence in both cyclin E and cyclin A that is required to localize them to the centrosome. It has been termed the centrosome localization sequence (CLS) (reviewed in (Pascreau et al., 2011)). The bulk of this work has been conducted using rat cyclins and Chinese hamster ovary (CHO) cells, but the CLS is highly conserved between rat, human and frog (Matsumoto and Maller, 2004).

The CLS is required for entry into S-phase, independently of CDK2 association and kinase activity (Matsumoto and Maller, 2004). Expression of a GFP-tagged WT-CLS fragment of cyclin E displaces endogenous cyclin E and cyclin A from the centrosome. Disruption of CLS-mediated localization of cyclin E and cyclin A results in a loss of other key factors from the centrosome, such as

MCM5 (Ferguson and Maller, 2008) and Orc1 (Ferguson et al., 2010). Loss of these factors at the centrosome leads to a block in the firing of DNA replication origins as indicated by a lack of Cdc45 and PCNA on chromatin. MCM2 is loaded properly indicating that the pre-replication complex is formed normally (Ferguson and Maller, 2010).

Cyclin E can be forced to localize to the centrosome even in the presence of GFP WT-CLS by fusing it to a conserved PACT (pericentrin - AKAP450 centrosomal targeting) domain (Ferguson and Maller, 2010; Ferguson et al., 2010). This restores localization of MCM5 to the centrosome as long as the cyclin E-PACT protein has an intact CLS. Using the PACT-domain to target cyclin E to the centrosome also restores DNA synthesis even though endogenous cyclin A and E are still displaced from their exact CLS-targets. This is an interesting observation in that it indicates that the mechanism of cyclin E action is based more on creating a locally high concentration of factors near the centrosome and not necessarily specific binding of cyclin E to the same target to which the GFP WT-CLS is bound.

This thesis will explore the role of the localization of cyclin E to the centrosome for promoting centrosome duplication. Using mutant forms of cyclin E to displace the endogenous protein from its native locations, and following centrosome duplication in live *Xenopus* oocyte extracts, we will determine if cyclin E must be localized to the centrosome by itself or in a complex with CDK2 to allow duplication.

CHAPTER II

Practical Aspects of Adjusting Digital Cameras

Introduction

Digital cameras have provided researchers with a tool that allows for nearly instantaneous image capture and display for presentation and quantitation that never existed before. Some of these cameras incorporate electron multiplication to enhance quantum efficiency and allow for the detection of fluorescent proteins that would never be detected using conventional film. Image processing software provides the power to enhance and analyze digitally recorded data. There is a danger, however, of forever degrading your data by improper use of digital cameras.

The purpose of this chapter is to introduce the adjustment of digital camera settings and use of the tools found within image acquisition software. Here we have reviewed and updated some previously written material in order to provide a treatment of the subject for those using digital cameras (Hinchcliffe and Sluder, 1998). The theme of this chapter is how to use camera image acquisition and display settings to optimize image contrast without irreversibly losing grayscale information.

Measuring Gray-Level Information

The pixel values in an image can be measured within many image capture software programs in two ways. The first is a histogram of pixel gray values and the second is a line-scan plot across a selectable axis of the image.

Understanding how to evaluate the information presented by these tools is critical

for properly adjusting the camera to maximize the image contrast without losing grayscale information. For simplicity, we will work with the 0–255 grayscale resolution of an 8-bit camera; the concepts are the same for cameras of any bit depth.

The Histogram

The histogram presents the number of image pixels (ordinate) as a function of gray level (abscissa) for the whole image or a region of interest. For an 8-bit camera, the pixel gray levels range from 0 on the left to 255 on the right. Figure 2.1.B shows the histogram of the entire image shown in 2.1.A (a differential interference contrast (DIC) image of several cultured mammalian cells). The sharp peak about one-third of the way from the origin indicates that the majority of the pixels in this image range from gray levels 40 to 110 with relatively few pixels of higher and lower values. It is important to note that the histogram is heavily weighted toward the background of the field (area around the cells) and that the brighter and darker portions of the specimen detail are represented in the histogram “tails” to the right and left of the main peak. For setting the camera acquisition and display parameters, these are the histogram values of interest, not just the primary peak.

The Line Scan

Most software packages allow the user to draw a line across a selectable

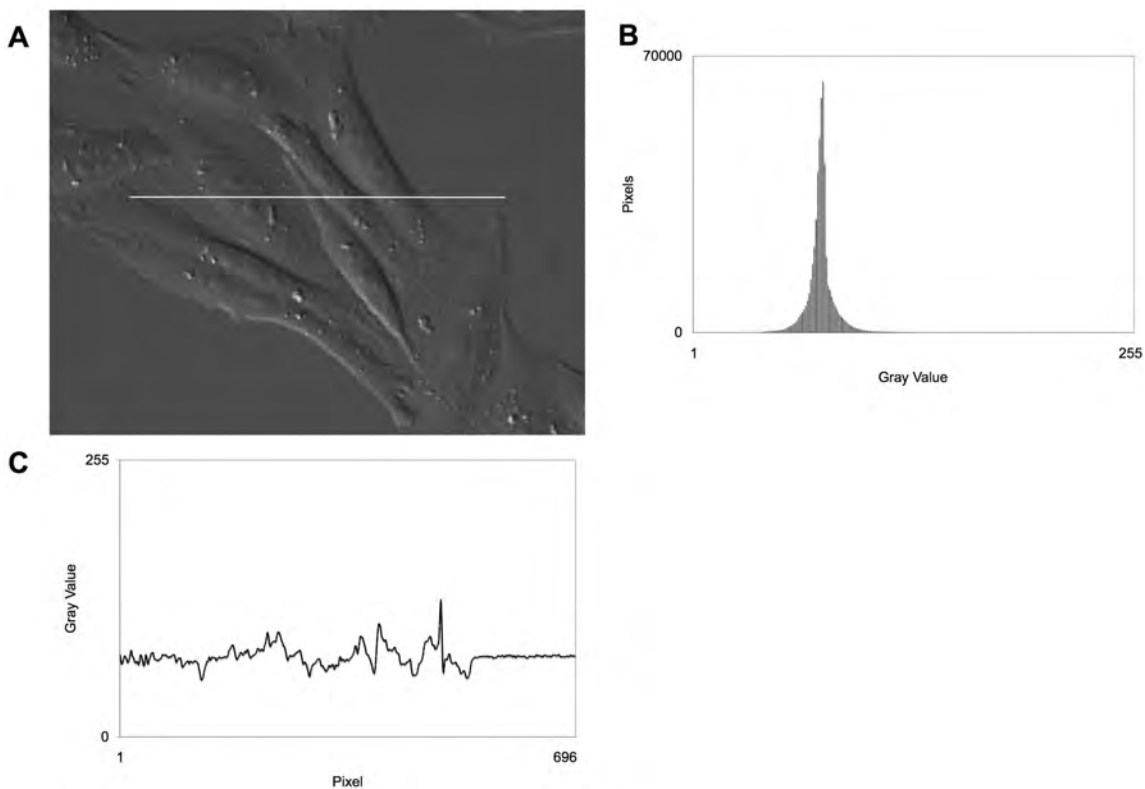


Figure 2.1 - Two ways to measure pixel gray values. Panel A is a differential interference contrast (DIC) image of cultured mammalian cells. Panel B shows a pixel gray-level histogram with the gray values ranging from 0 to 255 along the x-axis and the pixel number for each gray value shown on the y-axis. The histogram represents all pixels in the image. Panel C is a plot of pixel gray levels along the line scan shown in panel A. The x-axis is the pixel position along the line, and the y-axis represents gray values from 0 to 255. Usually, the position and orientation of the line can be user defined.

part of the image and measure pixel gray levels along that line. Many such packages enable the user to draw an arbitrary line rather than lines confined to the camera's horizontal and vertical axes. The readout is a graph that shows pixel location along the x-axis with the corresponding gray value on the y-axis, ranging from 0 to 255. Figure 2.1.C shows a line-scan plot of the gray levels found along the line seen in Figure 2.1.A. The line scan is particularly useful because the user can access the intensity information for any pixel of interest. This, as we will describe in the next section, allows the operator to know exactly how the adjustments made to the camera are applied to each pixel along the scan line.

While the information from a histogram is sometimes more difficult to interpret than the line scan, a histogram is often present in the corner of the display screen, and is updated in real time while the user is making imaging adjustments. The line-scan function usually requires an extra step to capture the image and measure the intensities afterward, making live adjustments difficult.

Other Strategies

In addition to the histogram and line-scan functions for determining proper camera settings, some software packages offer a tool that detects over- and underexposed pixels for the user. These pixels are displayed in a color overlay on the monochrome image being captured. Some software packages even allow

the user to choose how many gray levels below white or above black will be detected and displayed. Pixel colorization is an easily visible measure of camera performance.

Camera Settings

Exposure Time

Just as with a film camera, the exposure time setting determines how long the photoreactive element (here the CCD chip) is exposed to the light from the microscope. The result of underexposing is an image with a low signal-to-noise ratio. Overexposure will lead to saturated pixels within which there will not be any detectable image detail. Also, saturation of pixels can lead to an effect known as “blooming”(Fellers et al., 2005). When blooming occurs, adjacent pixels can also acquire signal leading to degradation of specimen detail in that region. Therefore, care must be taken to determine a proper exposure time that provides an image that is neither under- nor overexposed before adjusting any of the camera parameters as described below.

Offset

The offset control (sometimes referred to as “brightness” or “black level”) allows one to add or subtract an adjustable value from all pixels in the image. Normally, this is used to set the darkest portion of the specimen detail from some gray value down to a level close to zero when stretching the contrast in a low

contrast image (described below). The effects of changing the offset are shown in Figure 2.2. Figure 2.2.A, bottom panel, shows a gray scale ranging from 0 to 255 with the corresponding line-scan plot of this gray scale in the top panel. Figure 2.2.B shows what happens when the offset is made more negative; the lowest four gray values are driven to zero and the others are correspondingly reduced. Any specimen information contained in the lowest four gray levels is lost from the image. Figure 2.2.C shows the consequence of increasing the offset; the highest four gray levels are driven to white and the other values are correspondingly increased. Any specimen information contained in the highest four gray levels is lost from the image. The effect of driving pixel intensity values off-scale is often referred to as “clipping.”

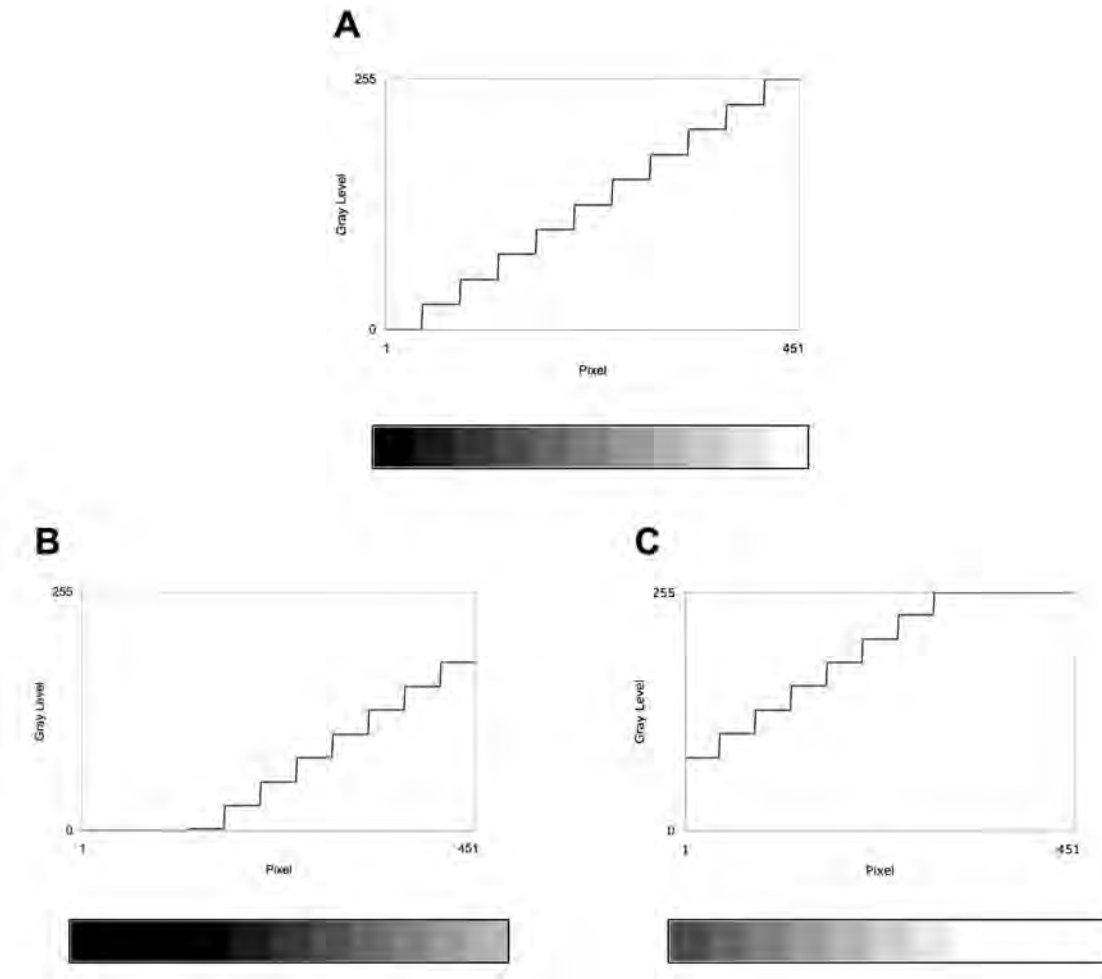


Figure 2.2 - Adjusting camera offset. Top panels are line scan plots of the grayscale test patterns shown in the bottom panels. The y-axis shows gray level ranging from 0 to 255 and the x-axis shows position across the image. Panel A shows the original image of the grayscale test pattern that includes the entire 256 gray-level range. Panel B shows what happens to the image and its line scan when the offset is decreased so that the fourth lowest gray value has been set to 0. Panel C shows what happens when the offset is increased such that the fourth highest gray level is set to 255—that is white. Notice that varying the offset does not alter the difference between each gray value.

Gain

Camera gain acts as an amplifier that varies the output value from the camera for a given change in input. It is expressed as a ratio of the number of electrons from the CCD chip that are converted into analog-to-digital units (ADU). Increasing the camera gain effectively means reducing the number of electrons required to produce one ADU (Roper Scientific, 2006). The effect this has on the captured image is to multiply all pixel values by the same value. For example, if two pixels initially have a difference of 5 gray values (say 45 and 50), increasing the gain multiplies all gray values by the same factor (say, 3); the new values of the pixels are 135 and 150—a gray value difference of 15.

Figure 2.3 shows the effects of changing camera gain on the grayscale test pattern. Panel A shows the full range of pixel gray levels ranging from black (0) to white (255). Figure 2.3.B shows what happens to the grayscale test pattern when one increases the gain. Notice that the differences between the output gray values increases and clipping of the higher gray values. When the gain is decreased, as shown in Figure 2.3.C, the differences between pixel gray values are decreased in the output. Although gray-level information is retained in principle, the resulting image is of low contrast. We also note that changing the gain does not alter the signal-to-noise ratio; both the signal and the noise in the camera signal are amplified.

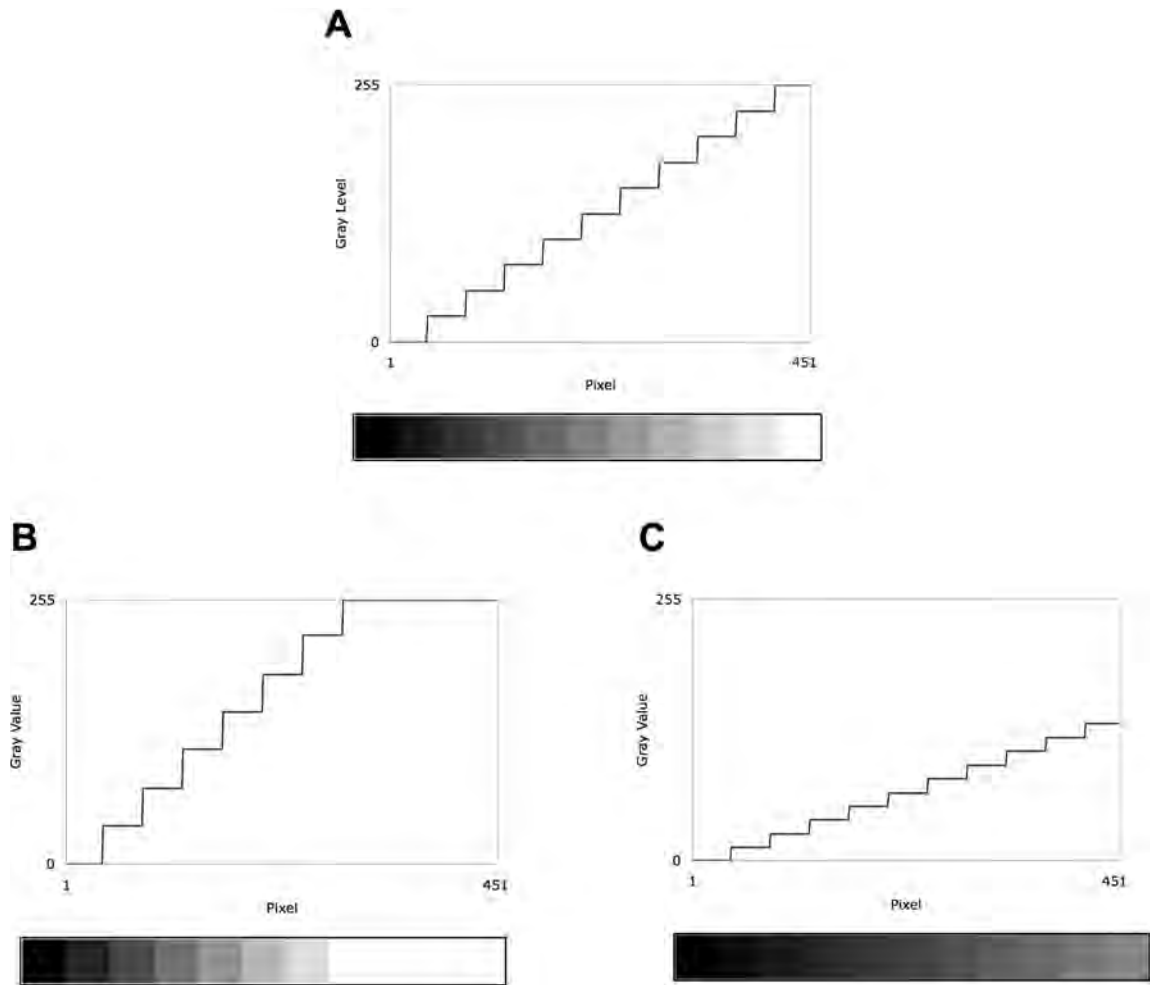


Figure 2.3 - Adjusting camera gain. Panel A shows the original image of the grayscale test pattern that includes the entire 256 gray-level range. Panel B shows what happens to the image and its line scan when the gain is increased. Notice that the differences between gray values (size of the steps) has been increased for all intensities (except 0). However, the highest gray values are now indistinguishable from each other because they have been “pushed” to saturation (255). In panel C, the gain has been decreased. While no gray values have been lost, it is more difficult to distinguish between gray values because the difference between steps has been decreased.

Contrast Stretching

Most real-life specimens are not represented by the entire 256 gray value range; often the specimen detail is found within a relatively narrow range of grays. By controlling exposure, offset, and gain, one can enhance the contrast and visibility of specimen detail without loss of essential gray-level information. In doing this, there are two primary considerations. First, one seeks to use the full dynamic range of the camera output and second, one does this for the specimen detail of interest. Specimen or background information not of interest can be allowed to saturate or go to black.

Setting the Exposure Time

Exposure is the light intensity per unit area at the detector multiplied by the amount of time the detector is exposed to the light. For a given exposure, one can use higher intensity illumination for a short time or a lower intensity for a longer time. The natures of the sample and the experiment will determine what combination of illumination intensity and exposure duration one will use. Regardless, one must use the histogram or the line-scan measurement tools to ensure that one does not saturate (drive to 255) pixels representing the brightest specimen details of interest and to ensure that there is adequate exposure to produce a gray level (>0) for the dimmest specimen detail of interest. Over- or underexposure can lead to irretrievable loss of specimen information. Obviously, the key consideration is the range of specimen gray levels, not necessarily the

gray level of the background. For example, when imaging a fluorescent specimen, one might not want to increase the exposure to the point that the background has a gray value, particularly if this means that the pixels representing the brightest specimen fluorescent intensity become saturated. Likewise, in a brightfield image of an absorbing specimen, one might allow the background values to saturate in order to capture the dimmest specimen detail.

Adjusting Offset and Gain

After an exposure time has been determined, the gray levels in the specimen detail of interest can be “stretched” to maximize the visibility of information captured. This is useful for images in which the specimen detail is represented by a relatively narrow range of gray values (i.e., a low contrast image of the specimen). The first step is to identify the specimen detail of interest that has the lowest gray value—even if it has a light gray value in the raw image. The offset is then adjusted to bring this gray level down to a lower gray-level value. Our example, shown in Figure 2.4, is a DIC image of cultured cells. Figure 2.4.A, left panel, shows the raw image with a line scan through one of the cells (white line). The pixel values along this line are shown in the right-hand panel. By reducing the offset, we set the lowest gray values to a value close to 0 (Figure 2.4.B). We also decrease the gray value of every pixel in the image, resulting in a similar line scan graph that is shifted closer to 0 on the y-axis.

The next step is to increase the gain to drive the lightest gray specimen

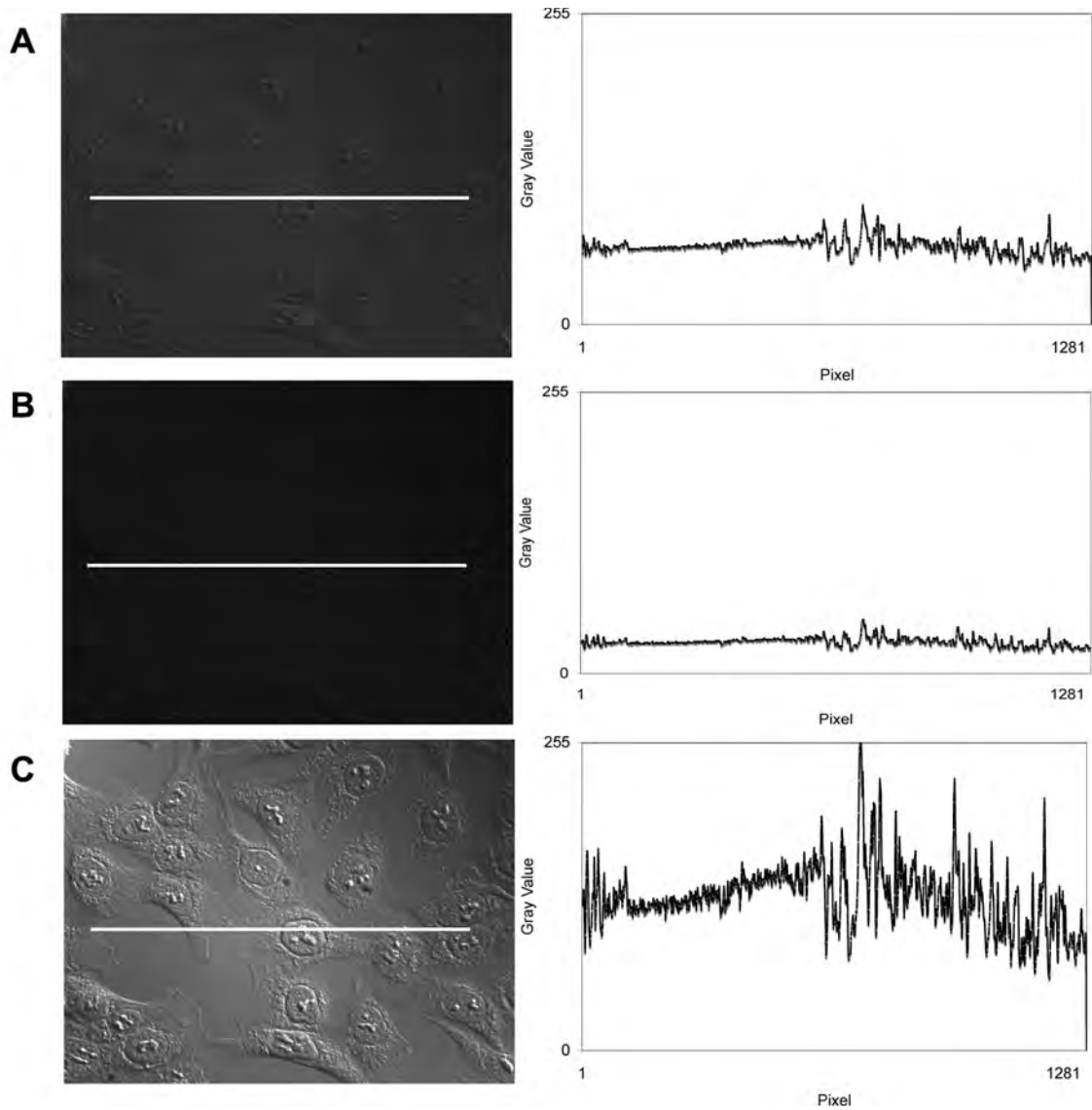


Figure 2.4 - Optimizing image contrast using the line scan plot. The left-hand panels are DIC images of fixed cells. The right-hand panels are line scan plots of pixel gray values along the line seen in each of the DIC images. Panel A shows an image with low contrast specimen detail. The corresponding line scan plot shows that the gray values of our image fall within a narrow range. Panel B shows the result of decreasing the offset. The gray values in the line scan plot are now closer to 0. In panel C, the gain has been increased so that the differences between the pixel values are increased. Notice that the highest specimen gray value in panel C is now close to 255. By making these adjustments, the range of pixel intensities for the specimen detail is now closer to the entire 256 gray value spectrum.

detail of interest to a value close to 255 as shown in Figure 4C. This multiplies all pixel values by the same factor thereby increasing the contrast between the highest and lowest values in the image. When done properly, this operation results in the conversion of an image of the specimen detail that starts with a limited range of gray values and represents it as an image that has the full range of gray values. Most importantly, there is no loss of essential gray-level information.

Figure 2.5 shows the contrast stretch operation conducted on the same specimen using the histogram of the pixel values of the entire image. In using the histogram display, it is important to bear in mind that the prominent peak of pixel values can be dominated by the background values and that the pixel values for the specimen detail may lie to the right and left of the peak. An extreme case is shown in Figure 2.6; panel A (left) shows a fluorescence image of a cell in which the objects of interest are centrosomes immunolabeled for γ -tubulin. The automatically scaled histogram of this image (panel A, right) shows that almost all the pixel values are close to zero with no values at lighter-gray levels. However, rescaling of the histogram (panel B) reveals that ~375 pixels are at 255 and their presence is difficult to detect with a single bar at the right margin of the histogram. Thus, the image of the centrosomes is saturated and substructure, if any, would not be detectable. The more important implication of finding these saturated pixels is that contrast stretching the prominent peak would not be of use. The histogram-scaling problem illustrated here can be

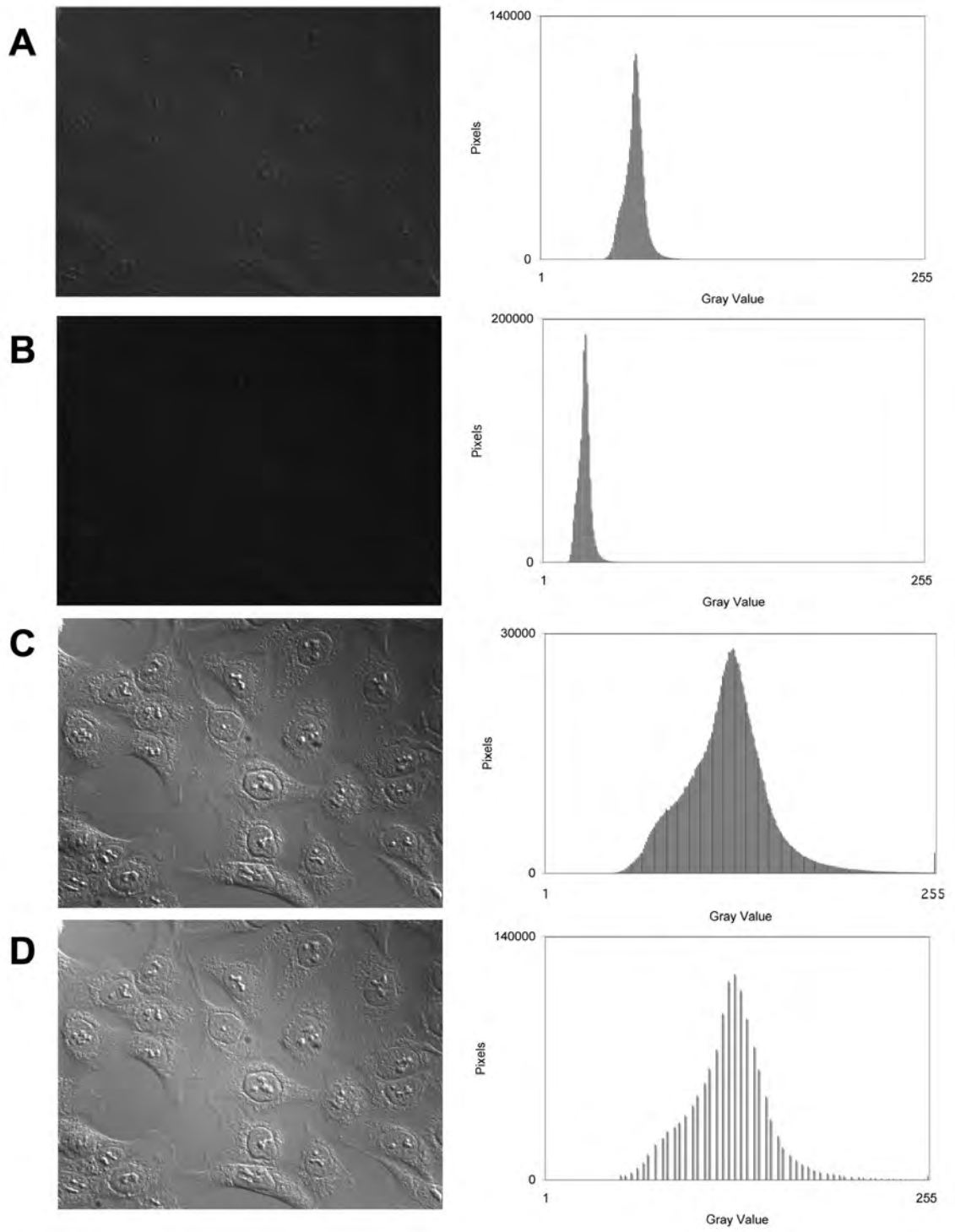


Figure 2.5 - Optimizing the image using the histogram. The left-hand panels are the DIC images of living cells used in Figure. 2.4. The right-hand panels are histograms of pixel gray values for the whole image. The adjustments made are identical to those in Figure 2.4. Panel A shows an image with low specimen contrast. The corresponding histogram shows that the image contains a narrow range of gray values. In panel B, the offset has been decreased. Note that all histogram values have been pushed closer to 0. In panel C, the gain has been increased so that the differences between gray values are increased producing a higher contrast image with, in principle, no loss of gray-level information. Note, however, that in this particular example, a few pixels have been driven to saturation as indicated by the small peak at the far right margin of the histogram. In a real-world situation, one would decide whether or not this is a problem. In panel D, the image in panel A has been contrast stretched using image-processing software after capture of the raw image. Note that the histogram in D has a gray-level range similar to that in C, but with fewer bars. This indicates a loss of grayscale resolution.

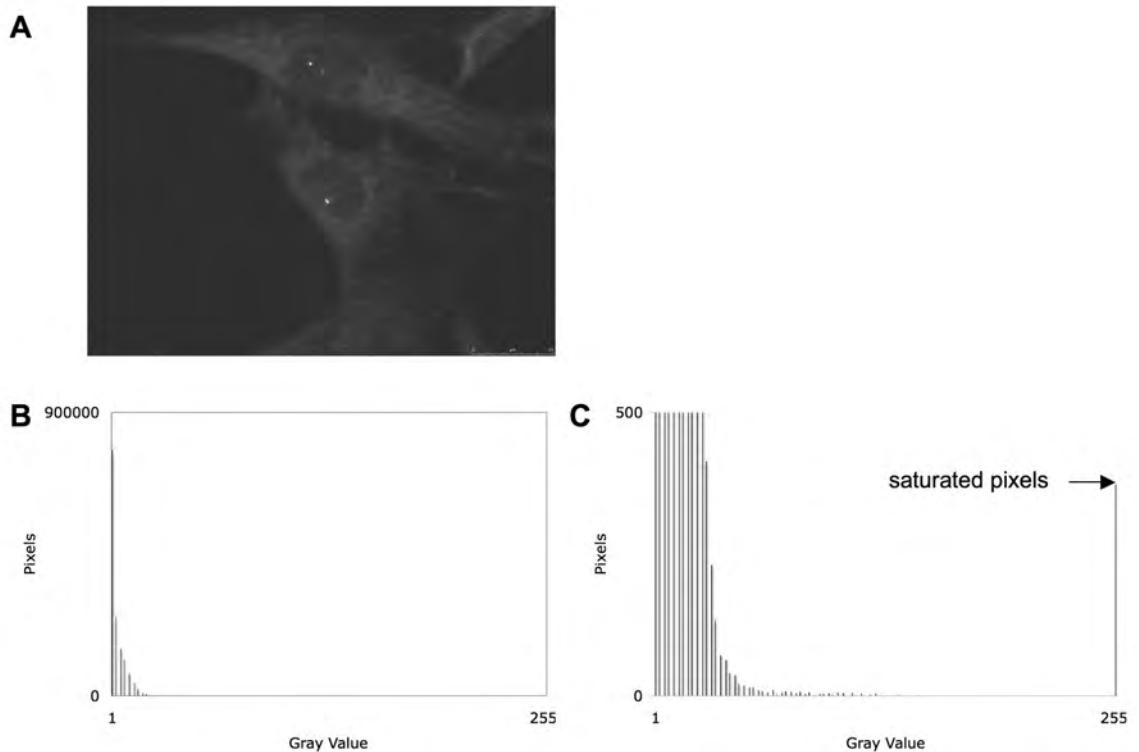


Figure 2.6 - The importance of scaling the y-axis of the histogram under some circumstances. Panel A (left) shows a fluorescence image of several cultured cells immunostained for γ -tubulin at the centrosomes (the two round, bright dots next to the nucleus). Panel A (right) shows the corresponding image gray-level histogram. All pixel gray values of the image appear to be concentrated near 0. Panel B shows the same histogram, but the scale has been changed from 0–450,000 to 0–500. Note that a number of pixels representing the γ -tubulin fluorescence are saturated (peak at far right margin of the histogram). If the centrosomes are the specimen detail of interest, one will have to decide if saturation of these pixels is acceptable or not.

addressed by using a histogram of a user-defined region of interest or by using a histogram with a logarithmic y-scale, an option found in some software packages.

Camera Versus Image Display Controls

An important distinction to draw is the difference between altering the camera's output parameters and the displayed image. In some software, one can only modify the characteristics of the camera output and consequently, the monitor display reflects the results. The image recorded to the hard drive also reflects the modifications made to the camera output.

In other image acquisition packages, one can independently vary camera output characteristics and the display characteristics. If modifications are made to the camera output, they are reflected in the monitor display and in the image that is recorded. However, if a contrast stretch is made through just the display controls, only the image on the monitor is modified. The raw image remains unaltered and the recorded image will not reflect any changes made.

Although it is possible to record the raw image and later conduct a contrast stretch, there is a penalty to be paid. For example, Figure 2.5.A–C shows the image gray-level histogram throughout the process of contrast stretching the image at the camera output level. Figure 2.5.D shows the same raw image that has been contrast stretched after capture using image-processing software. The histogram shows that the gray levels have been spread across approximately the same range of grays as in Figure 2.5.C. There are fewer bars, however,

indicating that fewer gray levels represent the image. In principle, this means that there is loss of gray-level resolution, particularly for 8-bit cameras (compare the histograms in Figure 2.5.C and D).

Since camera and display controls are not standardized, it is incumbent on the user to explore the options available in his/her software, understand what the controls modify, and proceed accordingly.

Chapter III

The good, the bad, and the ugly: Practical consequences of Centrosome Amplification

Abstract

Centrosome amplification (the presence of more than two centrosomes at mitosis) is characteristic of many human cancers. Extra centrosomes can cause the assembly of multipolar spindles, which unequally distribute chromosomes to daughter cells; the resulting genetic imbalances may contribute to cellular transformation. However, this raises the question of how a population of cells with centrosome amplification can survive such chaotic mitoses without soon becoming non-viable as a result of chromosome loss. Recent observations indicate that a variety of mechanisms partially mute the practical consequences of centrosome amplification. Consequently, populations of cells propagate with good efficiency despite centrosome amplification yet have an elevated mitotic error rate that can fuel the evolution of the transformed state. In this work we investigate the ways in which centrosome amplification degrades the fidelity of mitosis without leading to massive cell death from chromosome loss.

Introduction

As the primary microtubule-organizing center of the mammalian cell, the centrosome has a profound influence on all microtubule-dependent processes. When the cell enters mitosis, the daughter centrosomes nucleate the astral arrays that contribute most of the microtubules to the formation of the spindle. Through these astral microtubules, centrosomes determine spindle polarity, spindle position/orientation and the plane of cleavage. When mammalian somatic cells enter mitosis with extra centrosomes they are apt to assemble multipolar spindles and divide into more than two daughters (for examples see: Heneen, 1970; Heneen, 1975; Sluder et al., 1997). However, somatic cells also possess an alternative pathway that assembles bipolar spindles in the absence of centrosomes (Hinchcliffe et al., 2001; Heald et al., 1997; Levesque et al., 2003; Khodjakov et al., 2000). In this pathway, microtubules randomly assembled in the immediate vicinity of the chromatin are bundled into anti-parallel arrays by bipolar kinesins and the minus ends are moved distal to the chromosomes by chromokinesins. Minus-end-directed motor molecules, such as cytoplasmic dynein, move to and crosslink the minus ends of the microtubules to form a somewhat focused spindle pole, aided by the polar accumulation of the microtubule-bundling protein NuMA (Rieder et al., 2001; Compton, 2000; Karsenti and Vernos, 2001; Scholey et al., 2003). These two mechanisms for the organization of a bipolar spindle are not mutually exclusive and both appear to be

present in mammalian somatic cells. Nevertheless, when present, centrosomes are thought to act in a dominant fashion to determine spindle polarity (Nigg, 2002; Mazia, 1984; Hinchcliffe, 2001).

Results and Discussion

Centrosome amplification and cancer

In the whole organism multipolar mitoses can be dangerous, because the resulting loss or gain of chromosomes can lead to elimination of normal alleles for tumor suppressor genes and cause other genetic imbalances that can promote unregulated growth characteristics and a diminished apoptotic response to cellular damage (Tarapore and Fukasawa, 2002; Nigg, 2002; Orr-Weaver and Weinberg, 1998; Brinkley, 2001). Indeed, the cells of most late-stage human cancers are aneuploid, genomically unstable and show a high incidence of centrosome amplification (Lingle et al., 1998; Lingle et al., 2002; Pihan et al., 1998; Pihan et al., 2001; Tarapore and Fukasawa, 2002; Nigg, 2002; Brinkley, 2001; Duensing and Münger, 2002; Krämer et al., 2002). Genomic instability is thought to be a major driving force in multi-step carcinogenesis (D'assoro et al., 2002; Shono et al., 2001; Ried et al., 1999; Lengauer et al., 1998). For example, invasive breast cancers show a positive, linear correlation between centrosome amplification and aneuploidy (Lingle et al., 2002). Although it is not clear if centrosome amplification *per se* is sufficient to cause transformation (Nigg, 2002; Brinkley, 2001), centrosome abnormalities and aneuploidy are found in pre-invasive carcinomas and thus may be early events in cellular transformation (Pihan et al., 2003; Goepfert et al., 2002). Centrosome amplification is an intractable problem, because extra centrosomes are not eliminated and there is

no checkpoint that aborts mitosis in response to extra spindle poles (Sluder et al., 1997).

Practical consequences of centrosome amplification

The impression that centrosome amplification inevitably causes spindle multipolarity and grossly unequal chromosome distribution has become embedded in our thinking as a result of dramatic photographs in the literature of multipolar spindles in tumor cells, tumor cell lines and several cultured cell systems (for examples, see: Lingle and Salisbury, 1999; Fukasawa et al., 1996; Tarapore and Fukasawa, 2002; Heneen, 1970; Heneen, 1975; Sluder et al., 1997; Sato et al., 1999). However, this raises the question of how populations of tumor cells with extra centrosomes can propagate, even in the short term, in the face of substantial loss of genetic information through the distribution of chromosomes to multiple daughter cells. In the long term, even if a small fraction of the daughters survive, additional multipolar divisions should ultimately lead to loss of viability in the population. The disadvantage of extra centrosomes in cultured cells is illustrated by the finding that p53^{-/-} mouse embryo fibroblasts (MEFs) have ~30% incidence of centrosome amplification at early passages but that by passage 40 essentially all cells have a normal centrosome complement (Chiba et al., 2000). Obviously these concerns are at odds with reality; tumor cell populations do proliferate and, more to the point, the extent of centrosome amplification appears to increase progressively with advancing tumor stage

(Lingle and Salisbury, 2000; Lingle et al., 2002; D'assoro et al., 2002; Pihan et al., 2001; Ried et al., 1999; Skyldberg et al., 2001).

In theory, several mechanisms may act to moderate the practical consequences of centrosome amplification (Nigg, 2002; Brinkley, 2001). The important principle is that a population of cells with centrosome amplification must somehow avoid or get past a period of mitotic chaos and regain mitotic stability by re-establishing a bipolar spindle phenotype. First, it is possible that occasionally a daughter of a multipolar division will inherit only one centrosome and enough chromosomes to remain viable yet be genetically unbalanced. If cleavage failure is the source of centrosome amplification, the increased number of chromosomes may improve the chance that some daughters will have enough chromosomes to be viable. Over time, growth selection should favor the survival and proliferation of cells with normal centrosome numbers (Chiba et al., 2000). Second, cells might inactivate extra centrosomes. Although this remains a formal possibility, the only evidence for this phenomenon comes from the loss of the maternal centrosome in zygotes that show paternal inheritance of the centrosome used in development (Brinkley, 2001; Sluder 1992). We are aware of no convincing evidence for centrosome inactivation occurring in mammalian somatic cells that remain in the cell cycle. Finally, there may be selection within the population for cells with enhanced microtubule bundling activity that collects multiple centrosomes into two groups to form a functionally bipolar spindle. The classic example is the N115 cell line, which reliably bundles multiple

centrosomes into just two groups to form a bipolar spindle in mitosis (Ring et al., 1982). However, these are highly evolved cells that have developed strong compensatory mechanisms for centrosome amplification. For in vivo situations, one must ask how normal somatic cells, naive to supernumerary centrosomes, can survive a period of mitotic chaos long enough to allow for the selection of microtubule bundling activity that is sufficiently robust to bring multiple centrosomes together and thus allow bipolar spindle assembly.

The tenuous link between theory and the real-life behavior of cells prompted us to characterize the practical consequences of centrosome amplification for mitotic outcome in early-passage p53^{-/-} MEFs.

Examination of fixed interphase cells revealed that 34% contained more than two centrosomes (range 3–25 per cell), with no systematic correlation between centrosome number and passage number. For mitotic cells, those with two centrosomes assembled normal bipolar spindles, as expected (Figure 3.1.A). Some cells assembled multipolar spindles (Figure 3.1.B); telophase figures showing three or more groups of separated chromosomes indicate that such spindles distribute chromosomes in an unequal fashion (Figure 3.1.C). Other cells showed subtler but nonetheless significant mitotic defects. For example, Figure 3.1.D shows an example of a cell in which two partially separated

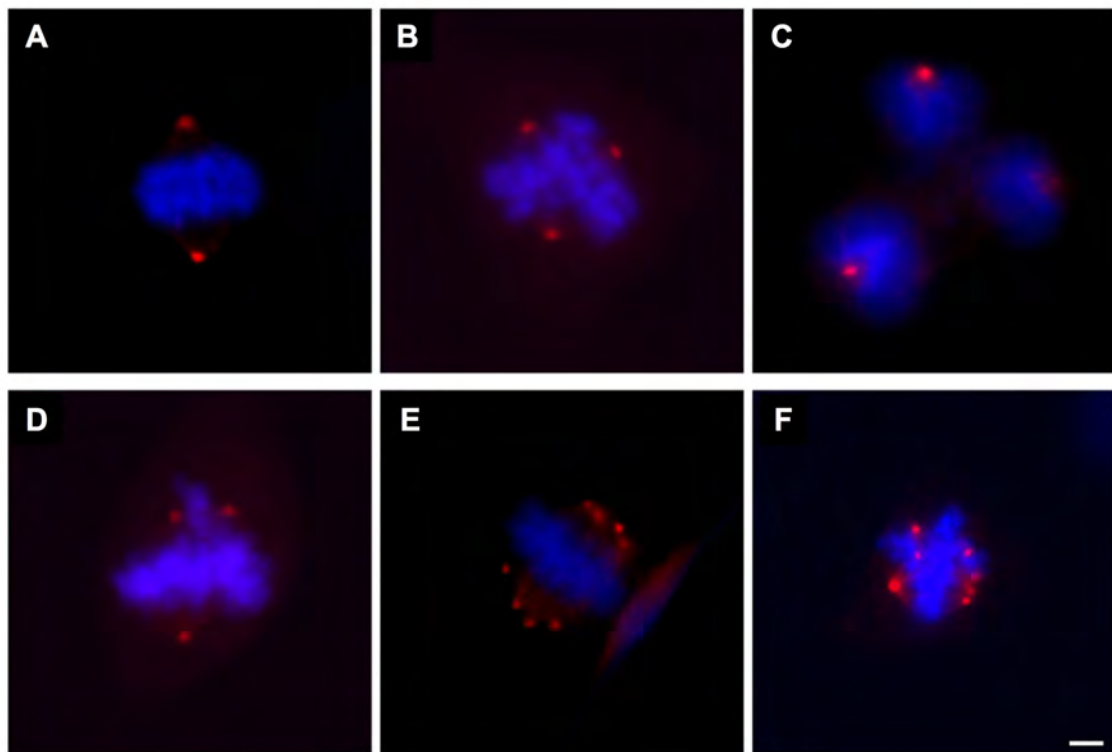


Figure 3.1 - Range of spindle morphologies in p53^{-/-} mouse embryo fibroblasts. (A) Normal bipolar spindle. (B) Tripolar spindle. (C) Tripolar spindle at telophase showing three-way chromosome distribution. (D) Spindle with two centrosomes at one spindle pole. One or more chromosomes are bioriented between the two upper centrosomes of this essentially bipolar spindle. (E) Bipolar spindle assembly with multiple centrosomes. (F) Multipolar spindle with three centrosomes bundled together at the lower right pole. Centrosomes are immunostained for gamma tubulin (red) and chromosomes are stained blue. Microtubule distributions are not shown.

centrosomes are present at one spindle pole. Although the bulk of the chromosomes are aligned on the metaphase plate, one or more chromosomes are bi-oriented between the incompletely separated centrosomes. Such cells may divide in a bipolar fashion if the incompletely separated centrosomes do not separate further, but the daughter cells will clearly not be genetically identical (also see: Tarapore and Fukasawa, 2002). This indicates that some mitoses will result in the gain or loss of one or a few chromosomes without a catastrophic loss of genetic information. Importantly, some cells showed an ability to assemble a bipolar spindle with multiple centrosomes at each pole (Figure 3.1.E) and would be expected to distribute chromosomes equally, at least for that division. Finally, some cells contained multipolar spindles in which some of the extra centrosomes were bundled at one or more of the spindle poles (Figure 3.1.F). This suggests that spindle pole bundling can be variable from cell to cell and perhaps variable from mitosis to mitosis. This may reflect a dynamic balance between the tendency of each centrosome to form its own spindle pole and the activity of proteins that bundle microtubules. Perhaps the extent of centrosome bundling depends upon the spatial proximity of centrosomes at the onset of mitosis; those close together will be bundled and those widely separated from the other centrosomes will establish independent spindle poles.

To examine the consequences of centrosome amplification for mitotic outcome directly, >200 live p53^{-/-} cells were followed through mitosis. With a *priori* knowledge that 34% of the population had extra centrosomes, it was

surprising that only 3.8% of the population (or ~10% of the cells with extra centrosomes) showed definite multipolar cleavages that formed separate daughter cells. Remarkably, 91.5% of the cell population divided in a bipolar fashion and the daughter cells reformed approximately equal-sized nuclei. Some of these cells showed a second shallow surface deformation in telophase that soon disappeared, ultimately resulting in bipolar division. Importantly, 4.7% of the cells completely failed cleavage. This was not simply the consequence of the culture conditions because all NIH 3T3 control cells (N=74) cleaved in a bipolar fashion. The mitotic results are summarized in Figure 3.2.

These observations reveal that the incidence of multipolar mitoses falls far short of the incidence of centrosome amplification. Several factors act singly or in combination to mute, but not eliminate, the effects of centrosome amplification. First, spindle-pole bundling in some cells leads to bipolar division with the extent of bundling determining whether chromosome segregation is equal (Figure 3.1.E) or almost equal (Figure 3.1.D). Second, when cells attempt a multipolar division only one furrow may persist, yielding two daughter cells containing possibly different chromosome complements. Although the daughter inheriting fewer chromosomes is at risk of being non-viable, the other daughter should have enough genetic information to continue propagating despite genetic imbalances. We speculate that the reason for the failure of all but one cleavage furrow is that cells have difficulty generating enough new surface area to complete more than one cleavage furrow consistently. In addition, cells with multipolar spindles

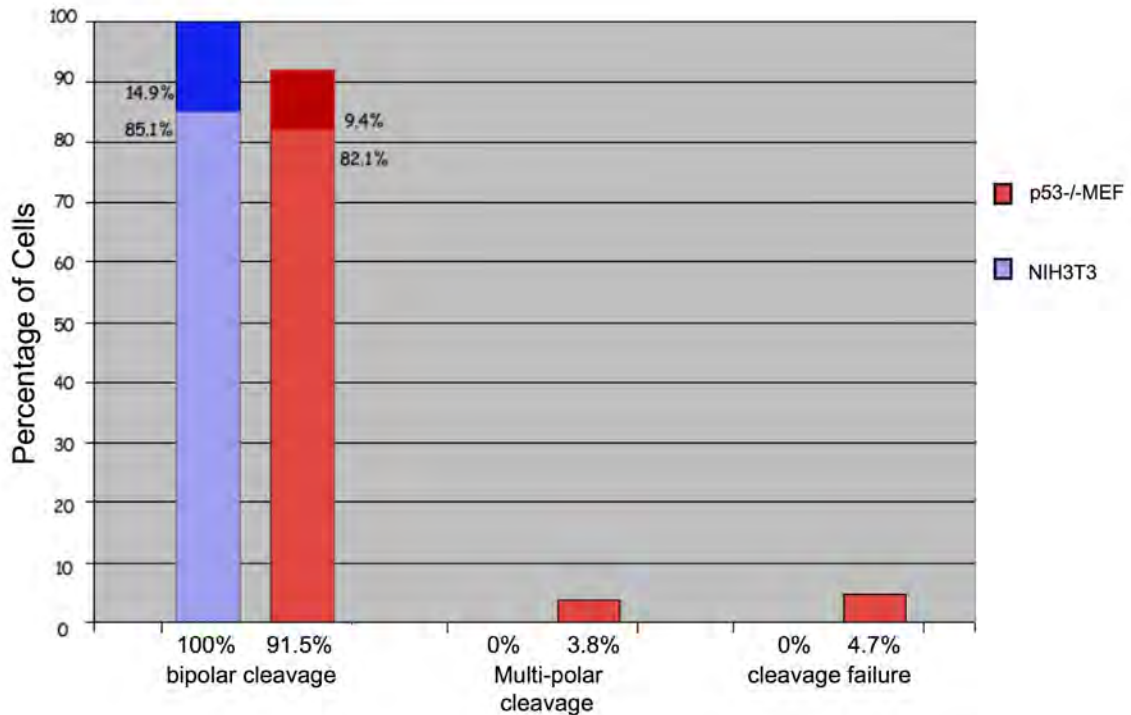


Figure 3.2 – Comparison of mitotic outcomes in p53^{-/-} MEF and NIH3T3 cells. In p53^{-/-} MEF cells, a total of 91.5% of cells ultimately divided in a bipolar fashion. Additional furrows appeared and regressed in 9.4% of the total population (n=213). NIH3T3 cells are cells of mouse origin and were used as a control. All NIH3T3 (n=74) cells divided in a bipolar fashion. While 85.1% of cells underwent a simple, unequivocal bipolar mitosis, 14.9% showed an additional furrow that ultimately regressed. Multiple daughter cells resulted from 3.8% of the total p53^{-/-} MEF population (0% in NIH3T3) and cleavage completely failed in 4.7% (0% in NIH3T3).

sometimes have one or more chromosomes that remain in the spindle mid-zone during anaphase as a result of the merotelic attachment of the kinetochore to two spindle poles (Heneen, 1970; Heneen, 1975; Sluder et al., 1997; Cimini et al., 2001). If such chromosomes remain in the midbody, they will block the completion of cleavage. Together these factors may explain why almost 5% of the p53^{-/-} cells completely failed cleavage. Such furrow failure is not unique to p53^{-/-} MEFs; PtK cells and sea urchin zygotes with multipolar spindles often fail to complete all furrows ((Sluder et al., 1986; Savoian et al., 1999); C Rieder, unpublished; G Sluder, unpublished).

Spindle Pole Bundling in “Normal” Cells

Earlier we raised the question of how a normal cell can survive the initial multipolar division after a centrosome amplification event. To determine how cells naive to centrosome amplification handle centrosome amplification, BSC-1 cells were treated with cytochalasin-D to block cleavage and, after removal of the drug, individual bi-nucleated cells, each now containing four centrosomes, were followed through mitosis. BSC-1 cells consistently have normal centrosome numbers and consequently have not undergone selective pressure for the ability to manage multiple centrosomes at mitosis. Importantly, these cells do not have a functional checkpoint that monitors polyploidy; all bi-nucleates entered mitosis. 44% divided in an indisputable tripolar or tetrapolar fashion (Figure 3.3.A, right-hand cell). Another 26% initiated a clear multipolar cleavage but in the end

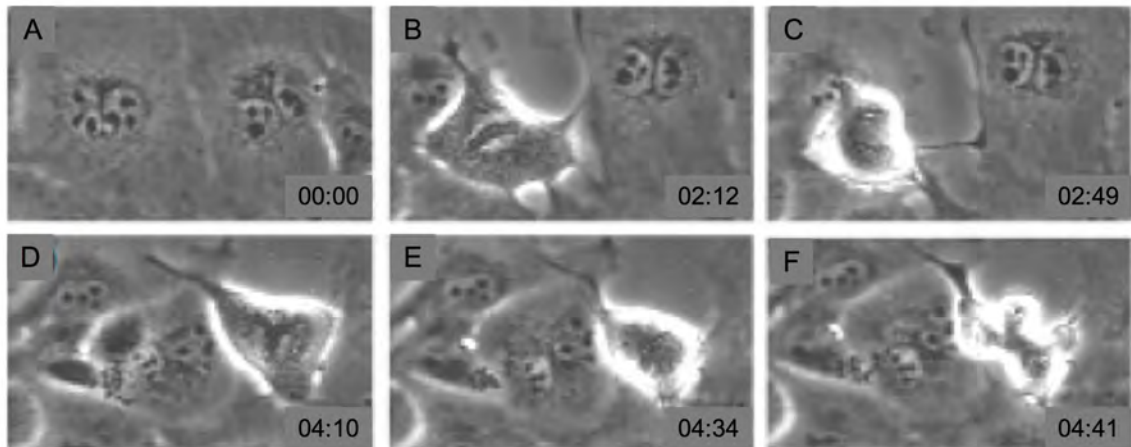


Figure 3.3 - Mitosis in two adjacent binucleate BSC-1 cells, each containing four centrosomes. (A) Both cells are in interphase with paired nuclei close together. (B) Left-hand cell has entered mitosis and assembled a bipolar spindle. Chromosomes aligned on a single metaphase plate are shown here in very early anaphase. (C) Late anaphase for left-hand cell; the daughter chromosomes are separated into just two groups. (D) Right-hand cell has assembled a tripolar spindle in mitosis. The chromosomes are aligned on a Y shaped metaphase plate. The left-hand cell has returned to interphase and the cleavage furrow has failed to complete so that both nuclei have come together. (E) Early anaphase in right-hand cell; chromosomes are being distributed to three poles. (F) Right-hand cell is cleaving into three daughter cells. Phase-contrast microscopy is used throughout. Hours and minutes after the first image are shown in the lower corner of each frame.

divided into two cells. The remaining 30% formed a single metaphase plate and divided into two daughter cells (Figure 3.3.D-E, left-hand cell). Thus, the 'bundling' of multiple centrosomes to allow bipolar spindle assembly in p53^{-/-} MEFs (and presumably tumor cells) is not simply due to clonal selection for cells that acquire special properties. Even cells naive to centrosome amplification can divide in a bipolar, albeit not necessarily equal, fashion some of the time when they contain extra centrosomes. Perhaps it is the acentrosomal spindle assembly pathway that organizes microtubules into a bipolar array that mediates this native bundling activity.

Conclusions

The often-stated notion that centrosome amplification causes aneuploidy and genomic instability simply by causing the assembly of multipolar spindles, although correct, is only part of the story. In practice, centrosome amplification does not have a simple or predictable effect on mitosis, nor does it necessarily lead to massive cell death through mitotic chaos. Rather, it causes highly variable outcomes of mitosis: some cells partition chromosomes equally, others mis-segregate one or a few chromosomes, and some fail cleavage. This variability is due to a dynamic balance between three factors: the tendency for each centrosome to form a spindle pole, spindle pole bundling, and the failure of all but one cleavage furrow, which favors a bipolar, but not always equal, mitotic outcome. Complete cleavage failure is particularly dangerous for the organism because it doubles the number of chromosomes, which enhances the chance that some daughter cells will have enough chromosomes to remain viable despite genetic imbalances. Indeed, tetraploidization often precedes aneuploidy in solid tumors (Levine et al., 1991; Galipeau et al., 1996; Shackney et al., 1989; Southern et al., 1997). Also, somatic cells may immediately tolerate, to a variable extent, a centrosome amplification event. Together, these compensatory factors functionally mute the practical consequences of spindle multipolarity so that mitotic chaos is reduced and the fidelity of the mitotic process is only partially degraded. The net result is that a population of cells will continue to propagate, despite some cell death (Fukasawa et al., 1997), yet will have an elevated level

of mistakes in chromosome distribution that can fuel the evolution of unregulated growth characteristics. Over time, Darwinian evolution will favor cells that have developed an increased ability to manage multiple centrosomes and thus regain some measure of mitotic stability.

Materials and Methods

Cell Culture:

P53 knockout mouse embryonic fibroblasts (p53^{-/-}-MEF) were a generous gift from Dr. Stephen Jones at the University of Massachusetts Medical School, Worcester, MA. NIH3T3 cells were a generous gift from Dr. Yu-Li Wang, also of the University of Massachusetts Medical School. All cells were grown in a humidified incubator at 37°C, 5% CO₂. MEF cells were grown in DMEM with 25mM HEPES, 15% fetal calf serum, 1% penicillin/streptomycin. NIH3T3 cells were grown in DMEM, 11mM HEPES, 10% donor calf serum, 2mM glutamine.

Live Cell Imaging:

Cells were prepared for live-cell imaging as previously described (Sluder et al., 2007). Briefly, cells were grown on 22mm square #1.5 coverslips. Coverslips were mounted onto aluminum frame using high vacuum silicone grease (Dow Corning, Midland, MI). Cells were observed using Zeiss Universal (Carl Zeiss Microimaging, Thornwood, NY) or Olympus BH2 (Olympus America, Center Valley, PA) microscopes using 10x phase-contrast objectives. Microscopes were maintained at 37°C in cardboard boxes heated by a proportional heat control system (Omega Engineering, Stamford, CT). Images were acquired with a Hamamatsu C2400 CCD camera (Hamamatsu Photonics, Bridgewater, NJ) using Adobe Premiere 4.0 (Adobe Systems Inc., San Jose, CA) (Hinchcliffe et al., 2001; Uetake and Sluder, 2007).

Immunofluorescence:

Cells on coverslips were fixed in -20°C methanol for 5 minutes, washed in PBS for 5 minutes and then incubated in blocking buffer (PBS, 1% BSA, 0.5% Tween-20) for 1 hour at room temperature. Antibodies were diluted into blocking buffer at the dilutions listed below. Antibody incubations (primary: mouse anti- γ -tubulin (GTU-88) at 1:1000; secondary: goat anti-mouse AlexaFluor 594 at 1:1000) were carried out by inverting coverslip onto a $100\mu\text{l}$ drop of diluted antibody on Parafilm for 1 hour at 37°C . Between antibody incubations, coverslips were washed 3 x 10 minutes in blocking buffer at room temperature. The coverslips received one final wash in PBS containing $2\mu\text{g/ml}$ Hoechst 33342 (to label DNA) for 5 minutes at room temperature before mounting onto slides on a $7\mu\text{l}$ drop of 1:1 glycerol in PBS and sealed with clear nail polish.

Chapter IV

The Importance of the Centrosomal Localization Sequence of Cyclin E for Promoting Centrosome Duplication in *Xenopus* Extract

Abstract

The centrosome is the major microtubule-organizing center for the cell. The number of centrosomes at mitosis determines the number of spindle poles to which the chromosomes will segregate at anaphase. Thus, proper control of centrosome duplication is of utmost importance to the fidelity of mitosis. The late G1 rise in CDK2/cyclin E activity coordinately initiates DNA replication and centrosome duplication. Recently, a 20 amino-acid sequence was identified in cyclin E that was shown to be required for localization of cyclin E to the centrosome and for entry into S-phase in CHO cells. We used an S-phase arrested *Xenopus* egg extract to test if CLS-mediated targeting of cyclin E is required for centrosome duplication. We also investigate whether cyclin E targeting alone is sufficient to promote centrosome duplication, or if it must be in a complex with CDK2. We found that expression of a cyclin E mutant deficient in CDK2 binding acted in a dominant negative fashion to block centrosome duplication. These observations indicate that soluble CDK2/cyclin E activity is not sufficient to initiate centrosome duplication; the kinase complex must be targeted to substrates presumably on the centrosome to promote duplication. The mechanism of cyclin E targeting to its substrates via the CLS provides a possible explanation of how centrosome duplication could be tightly controlled in the face of high cytoplasmic CDK2/cyclin E activity.

Introduction

Centrosome duplication is a critical step in the cell cycle that has a direct impact on the success or failure of chromosome segregation and cell division. During S-phase, the centrosome must be duplicated once and only once so that the cell has two centrosomes upon entering mitosis. During mitosis, the centrosomes act as the poles of the mitotic spindle, the microtubule-based machinery responsible for segregating chromosomes to the resulting daughter cells. Having too many centrosomes in mitosis leads to genomic instability by the formation of multipolar spindles that either result in true multipolar divisions or in an increased incidence of lagging chromosomes (Ganem et al., 2009; Sluder and Nordberg, 2004). Proper control of the duplication process is thus of extreme importance to ensure the fidelity of mitosis and genomic stability.

CDK2/cyclin E activity has been shown to be required for initiating the centrosome duplication process (Hinchcliffe et al., 1999; Lacey et al., 1999; Freed et al., 1999). Recently a 22 amino acid sequence in cyclin E, conserved in rat, mouse, human, and frog, has been shown to be required for centrosomal localization of the cyclin E protein and has been dubbed the Centrosomal Localization Signal (CLS) (Matsumoto and Maller, 2004). CLS-dependent localization of cyclin E has been shown to be required to enter S-phase (Matsumoto and Maller, 2004), specifically for localizing MCM5 to centrosomes (Ferguson and Maller, 2008) and loading the DNA replication factors Cdc45 and PCNA (Ferguson and Maller, 2010) onto DNA.

There are many similarities between DNA replication and centrosome duplication. Both occur during S-phase, promoted by a coordinate rise in CDK2/cyclin E activity. Both processes are tightly regulated, once and only once events. And both are semi-conservative duplications where the original structure is preserved while serving as a template for the new. We wanted to test if spatial localization of cyclin E to the centrosome is required for centrosome duplication in a fashion similar to its requirement for S-phase entry (Matsumoto and Maller, 2004), something that heretofore has not been tested.

Subcellular regulation of CDK2/cyclin E activity would prove useful in embryonic systems where it is known that cyclin E protein levels are constitutively high throughout many of the early cell cycles (Schnackenberg et al., 2008; Sumerel et al., 2001; Rempel et al., 1995; Hartley et al., 1996). How is centrosome duplication tightly regulated when the overall cellular cyclin E levels and CDK2 activity responsible for initiating duplication is constitutively high and not directly controlled via transcriptional or translational regulation?

We tested whether CLS-mediated localization of active CDK2/cyclin E complexes to the centrosome is required to promote duplication. We used a cytoplasmic extract made from *Xenopus* oocytes, arrested in S-phase, that supports multiple rounds of centrosome duplication (Hinchcliffe et al., 1999). Using time-lapse polarized light microscopy, we directly observed centrosome duplication dynamics in the presence of several mutant cyclin E proteins. We introduced mRNA coding for a cyclin E mutant (R128A) that is deficient in CDK2

binding, has a functional CLS and has been reported to displace endogenous CDK2/cyclin E complexes from the centrosome (Matsumoto and Maller, 2004). We compared the R128A results to the centrosome duplication characteristics in the presence of a double-mutant cyclin E (SW/RA) that does not localize to the centrosome or bind CDK2.

Our methods allowed us to determine that cyclin E localization at the centrosome was not sufficient to promote centrosome duplication, as it is for entry into S-phase (Matsumoto and Maller, 2004). Our results indicate that centrosomal cyclin E needs to be complexed with CDK2 in order to promote centrosome duplication.

Results

Cycling *Xenopus* extracts arrested in S-phase with Aphidicolin that support multiple rounds of centrosome duplication were prepared as previously described (Hinchcliffe et al., 1999). We tracked centrosome duplication by following the doubling of the microtubule asters nucleated by centrosomes in continuous time-lapse image sequences. In the polarized light microscope, the radial array of microtubules (aster) appears as a small star with light and dark quadrants (Figure 4.1.A-C). Example frames from the beginning (4.1.A), middle (4.1.B), and end (4.1.C) of a movie of a control extract show the steady increase in aster number over time.

We followed individual asters and their progeny over the course of the experiment and determined the exact fate of each input aster. Each aster has three possible fates – it can double, it can be lost from the field of view, or it can reach the end of the film sequence without doubling. In scoring duplication we counted only asters whose lineages were followed throughout the entire experiment. Any asters that went out of the field of view, or out of the plane of focus, were discarded (Figure 4.1.D).

In a typical control extract, we observed up to 4 aster doublings from the starting aster over the course of six hours. The first doubling of the input aster happens within about 30 minutes of the start of the experiment (data not shown) and represents the separation of the pair of centrioles brought in with each sperm nucleus; followed by their duplication (Figure 4.1.D). We therefore did not count

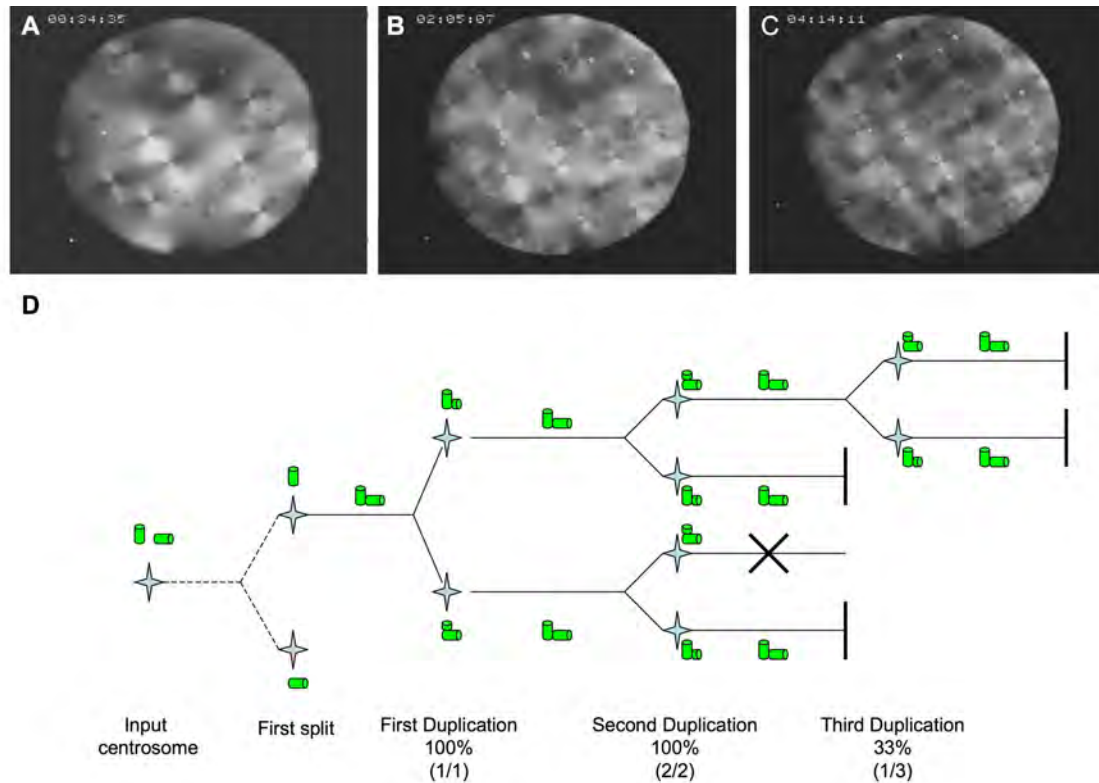


Figure 4.1 – Quantifying centrosome duplication using Polarization Microscopy. (A-C) Representative images from a time-lapse series of a water control experiment (time is hh:mm:ss). Panel A shows few asters in the field at 00:34:35 while Panels B and C show an increase in asters over time (02:05:07 and 04:14:11 respectively). (D) An example of a single centrosome lineage. The first observable doubling of a microtubule aster is the splitting of mother and daughter centrioles from the input sperm centrosome and is not counted in the data set. Subsequent aster doublings are scored as centrosome duplication events. If mother and daughter centrioles separate before duplication, procentrioles will form quickly (Loncarek et al., 2008a) (depicted as short centrioles in green at each aster). At each round of centrosome duplication, the time is recorded and the inter-duplication time is calculated (used in Figure 4.4). The ratio of centrosomes that duplicate to the number of centrosomes present at the beginning of a round is calculated and expressed as a percentage (see bottom row of panel D; used in Figure 4.3). Centrosomes that are lost from the field of view are indicated with an “X” and are discarded from the data set. Centrosomes that do not duplicate by the end of the image sequence are noted as “|.”

the first visible aster doubling in our analysis. Any subsequent aster doubling represents centrosome duplication. A study by Loncarek, et al. showed that the removal of a daughter centriole from the area adjacent to the mother induces the formation of a new daughter (Loncarek et al., 2008). That study suggests that single, unduplicated centrioles do not exist for long before a new daughter centriole is formed. A visible doubling of a microtubule aster would represent the splitting of two centrioles, followed by the immediate subsequent formation of new daughter centrioles. Therefore, we use aster doubling after the first split as an indicator of centrosome duplication.

Cyclin E mutant protein expression in *Xenopus* egg extracts.

To understand the kinetics of protein translation of our GFP-tagged mutant cyclin E constructs, messenger RNA for each of the mutants was added to S-phase arrested *Xenopus* extracts to a final concentration of 20ng/ μ l and the extract was incubated at 18°C for up to 6 hours. Samples (3 μ l) were taken at various time points and processed for SDS-PAGE and Western blot for GFP. Protein expression levels reached a maximum after approximately 1 hour (Figure 4.2.A). In a typical extract, the protein was expressed for at least 4 hours (Figure 4.2.B). If no GFP-tagged protein was expressed, the experiment was discarded.

Protein expression from the mRNA was variable from experiment to experiment. Figure 4.2.C shows samples of extract expressing R128A from

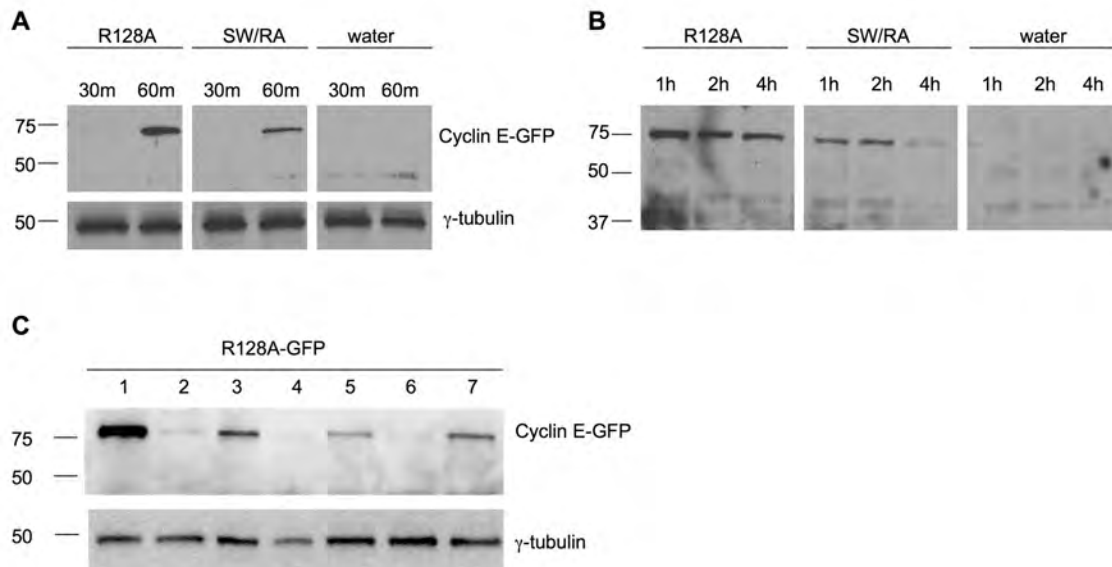


Figure 4.2 - Protein expression from mRNA in *Xenopus* extract. Samples of extract expressing GFP-tagged cyclin E mutants from 20ng/μl mRNA were separated using SDS-PAGE and probed with antibodies to GFP. Gamma-tubulin is shown as a loading control (A and C). (A) R128A and SW/RA mutant cyclin E protein expression is low at 30 minutes, but increases significantly at one hour. There is no visible GFP-tagged protein in the water control lanes. (B) Expression of R128A and SW/RA mutant cyclin E from mRNA stays high over the course of the experiment. The background bands at approximately 40KDa serve as loading control comparison. (C) Mutant cyclin E expression varies from day to day. Lanes 1-7 show samples from an R128A expression extract from seven different days' experiments. In each case the amount of mRNA added was the same as well as incubation time. Total protein in each lane is similar according to γ-tubulin control.

seven independent experiments. The amount of total protein loaded was nearly equivalent (see γ -tubulin loading control), however we saw clear differences in the amount of expressed protein from the R128A mRNA. Interestingly, we found that the experiments with the lower amounts of protein expression (lanes 2, 4, and 6) actually exhibited the lowest number of centrosome duplications.

Expression of R128A reduces the percentage of daughter centrosomes that duplicate.

We added mRNA coding for the full-length CDK2 binding mutant (R128A) cyclin E protein to S-phase arrested *Xenopus* extract and observed centrosome duplication. The mutation at R128A is analogous to S180D in rat cyclin E and is reported to properly localize to the centrosome, not bind CDK2, and have no associated kinase activity. It is also reported to displace endogenous cyclin E and cyclin A from the centrosome (Matsumoto and Maller, 2004; Ferguson et al., 2010). Expression of S180D does not affect S-phase entry in CHO cells (Matsumoto and Maller, 2004) and thus our extract should not have been driven out of S-phase arrest by R128A expression.

For each centrosome that duplicates, two daughters are formed; each has the capacity to duplicate in the next round, or not. We scored the percentage of centrosomes that duplicated at each round for each condition tested (Refer to Figure 4.1.D). We compared the results of each mutant (R128A or SW/RA) to the control extracts (water or luciferase).

All data were pooled from multiple independent experiments. Water control extract data were combined from 14 independent experiments. Luciferase mRNA control data were from 4 independent experiments. The R128A mutant data were compiled from 11 independent experiments while the SW/RA data were from 5 independent experiments. The n reported in each section is the total number of asters counted from all experiments.

Almost all centrosomes in all conditions duplicated in the first round (Figure 4.3 – Round 1). At the second round of duplication, we found 80.4% (n=225) of asters in the water control extract doubled again. In the presence of R128A, however, only 46.8% (n=263) of daughters duplicated a second time (Figure 4.3 – Round 2).

To test if the reduction in the percentage of centrosomes that duplicated was due to the over-expression of cyclin E, we expressed a double-mutant cyclin E (SW/RA) that has a mutated, non-functional CLS and does not bind CDK2. We chose to use this mutant instead of expressing WT cyclin E because the SW/RA mutant should not disrupt the interactions of endogenous cyclin E with CDK2 or the binding of the native kinase complex to the centrosome. In the presence of the SW/RA mutant, we observed a moderate reduction in daughter centrosome duplication to 59% (n=95) compared to controls (Figure 4.3 – Round 2) but not as great a reduction as seen in the presence of R128A.

To address the possibility that the reduction in centrosome duplication was due to non-specific effects of excess mRNA, we tested centrosome duplication in

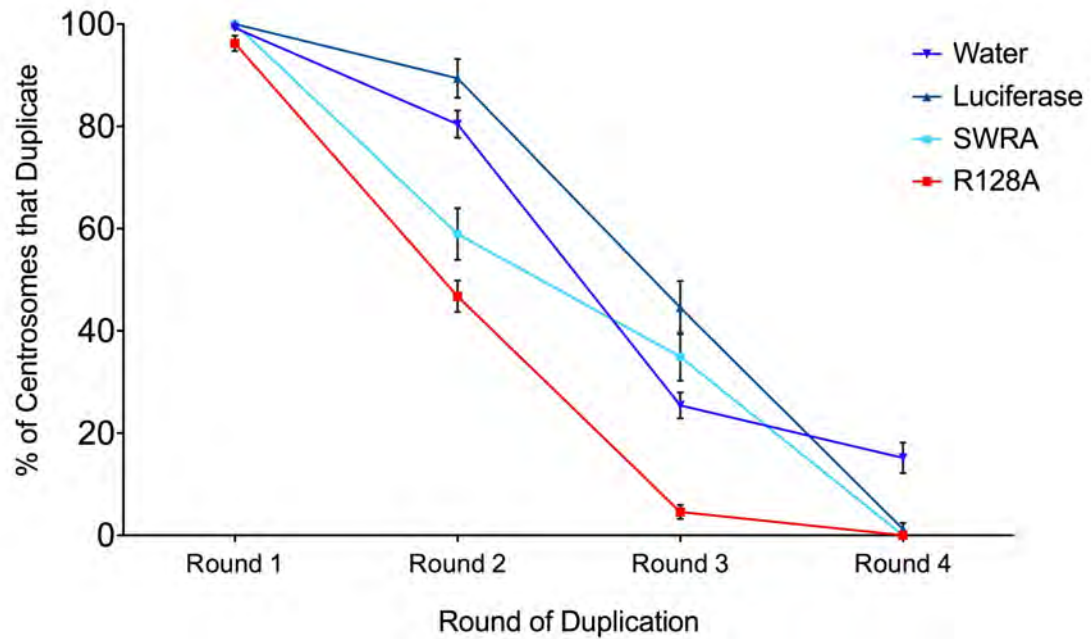


Figure 4.3 – Percentage of centrosomes that duplicate at each round. The percentage of centrosomes that duplicate at successive rounds was plotted (+/- standard error) for each condition tested: R128A, SW/RA, luciferase and water. Percentages were calculated as the ratio of centrosomes that duplicated to the total number of centrosomes that could be followed from the previous round of duplication. Centrosomes that were lost by either migrating out of the field of view or moving out of focus were not counted. For “Round 1” the percentage was the ratio of centrosomes that duplicated to the total number of input centrosomes visible in the field of view.

the presence of luciferase mRNA at the same concentration used for all other constructs (20ng/ μ l). Although luciferase protein was never expressed in *Xenopus* extracts (data not shown), the mRNA remained intact, as judged by agarose gel electrophoresis, and was expressed properly in parallel reticulocyte lysate assays (data not shown). Centrosomes in the presence of luciferase mRNA behaved similarly to water controls with 89.4% (n=66) of the daughter centrosomes having duplicated (Figure 4.3 – Round 2).

At the third round of duplication, in water and luciferase control experiments, daughter centrosomes duplicated 25.4% (n=299) and 44.6% (n=92) of the time respectively. Only 4.6% (n=240) of the daughters duplicated in the presence of R128A at this round. Interestingly, 35% (n=103) of the daughters in the presence of SW/RA duplicated a third time (Figure 4.4), which was nearly equivalent to the controls (Figure 4.3 – Round 3).

By the fourth round of duplication, only 15.1% (n=145) of water control and 1.2% (n=82) of luciferase centrosomes duplicated. No centrosomes duplicated a fourth time in the presence of R128A or SW/RA (Figure 4.3 – Round 4).

Expression of R128A reduces the average number of centrosome duplications

Centrosomes in control extracts duplicated 2.34 times on average over the course of a six-hour experiment (n=411) (Figure 4.4 – 2nd bar). In the presence

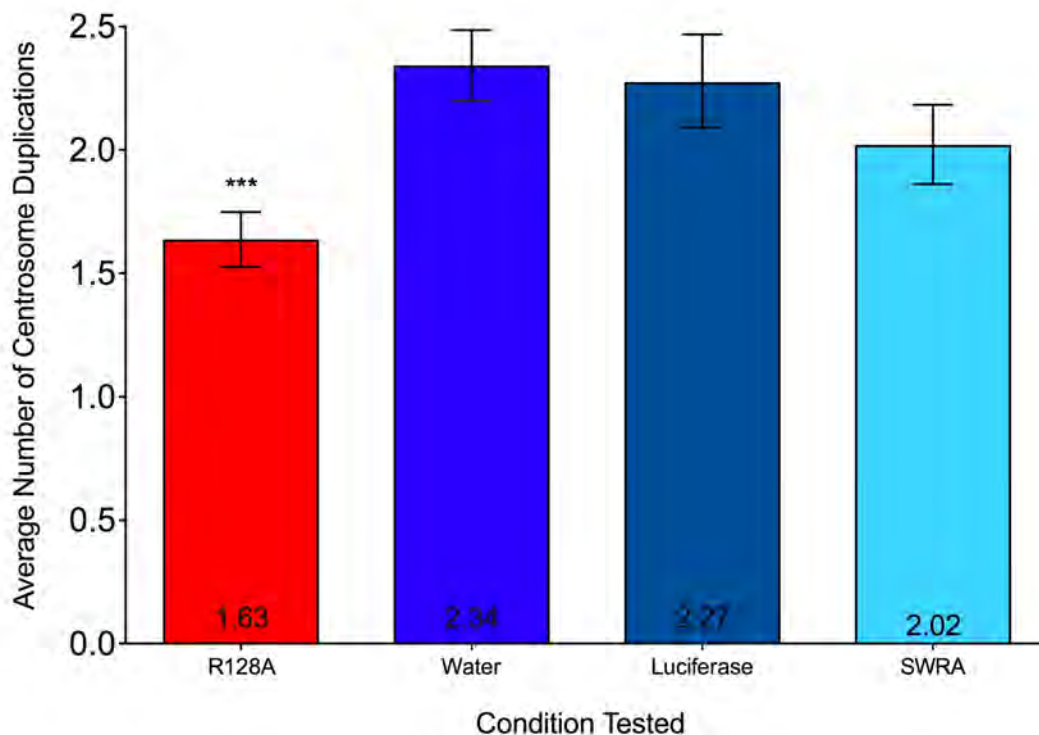


Figure 4.4 - Average number of centrosome duplications per 6-hour period. The average number of centrosome duplication events were calculated and displayed as mean +/- the 95% confidence interval. Asterisks denote significance compared to water control ($p < 0.0001$).

Comparison of Average Number of Centrosome Duplications

Comparison	Difference (percentage)	p-value
Water :: R128A	2.34 versus 1.63 (-30%)	<0.0001 (***)
Luciferase :: R128A	2.27 versus 1.63 (-28%)	<0.0001 (***)
SW/RA :: R128A	2.02 versus 1.63 (-19%)	0.0323 (*)
Water :: Luciferase	2.34 versus 2.27 (-3%)	0.9948
Water :: SW/RA	2.34 versus 2.02 (-14%)	0.1619
Luciferase :: SW/RA	2.27 versus 2.02 (-11%)	0.6944

Table 4.1 – Comparison of average number of centrosome duplications in a 6-hour period. Comparisons between each experimental condition are listed in the left hand column. The differences in centrosome duplications as displayed in Figure 4.4 are reported in the middle column and expressed as a percentage change. The p-value for each comparison is reported in the third column. The analyses were conducted using a Generalized Linear Mixed Model (GLMM) and the p-values are weighted accordingly.

of luciferase mRNA, centrosomes duplicated an average of 2.27 times (n=143) representing only a 3% difference ($p=0.9948$) (Figure 4.4 – 3rd bar; Table 4.1).

In extracts expressing R128A the average number of centrosome duplications dropped to 1.63 (n=384). This represents a 30% reduction in duplication compared to water controls ($p<0.0001$) (See Figure 4.4 – 1st bar; Table 4.1) and a 28% reduction in duplication compared to luciferase ($p<0.0001$) (Table 4.1).

In extracts expressing SW/RA the centrosomes duplicated an average of 2.02 times (n=178) versus 2.34 in control. This represented only a 14% reduction compared to the water control ($p=0.1619$) (Figure 4.4 – 4th bar; Table 4.1). We compared the R128A result to SW/RA and found that duplication in the presence of R128A was reduced by 19% ($p=0.0323$) (Figure 4.4 – 1st bar versus 4th bar; Table 4.1) compared to SW/RA.

Centrosome Duplication Timing

We compared the times from start of the experiment to the first duplication, and to subsequent duplications, between extracts expressing the mutant forms of cyclin E and the controls. We saw a significant increase in the amount of time to both the first and second rounds of centrosome duplication in the presence of the R128A mutant cyclin E compared to water and luciferase controls as well as compared to the SW/RA double mutant cyclin E.

In control extract (water), it took 92 minutes for the centrosomes to duplicate the first time. The luciferase mRNA control behaved similarly, taking 88 minutes for the centrosomes to duplicate. In the presence of R128A, it took 139 minutes; an increase of 43 minutes (47%) over the water control and 42 minutes (48%) over the luciferase control. We did not see this delay in the presence of the SW/RA double mutant cyclin E; centrosomes duplicated 103 minutes after the start of the experiment. This represented only a 7-minute (8%) delay versus the water control and a 6-minute (7%) delay versus luciferase. See Figure 4.5.A and Table 4.2 for a summary of the data.

The centrosome duplication delay in the presence of R128A persisted in the second round of duplication as well (Figure 4.5.B). Centrosome duplication was delayed by 30 minutes (34%) compared to water control and by 25 minutes (27%) compared to luciferase. By the third round of duplication, however, a delay was no longer observed between R128A and water or luciferase (Figure 4.5.C). Interestingly, the SW/RA mutant had a completely different timing pattern. Compared to water control, there was a delay of 22 minutes (25%) seen at the second round of duplication (Figure 4.5.B). However, the time to the third round of duplication was much faster compared to all other conditions at only 39 minutes (Figure 4.5.C).

Compared to all other conditions, the distribution of the times at which each centrosome duplicated was much greater in the presence of R128A (Figure 4.5.A-C) than the other conditions tested. This distribution spread was more

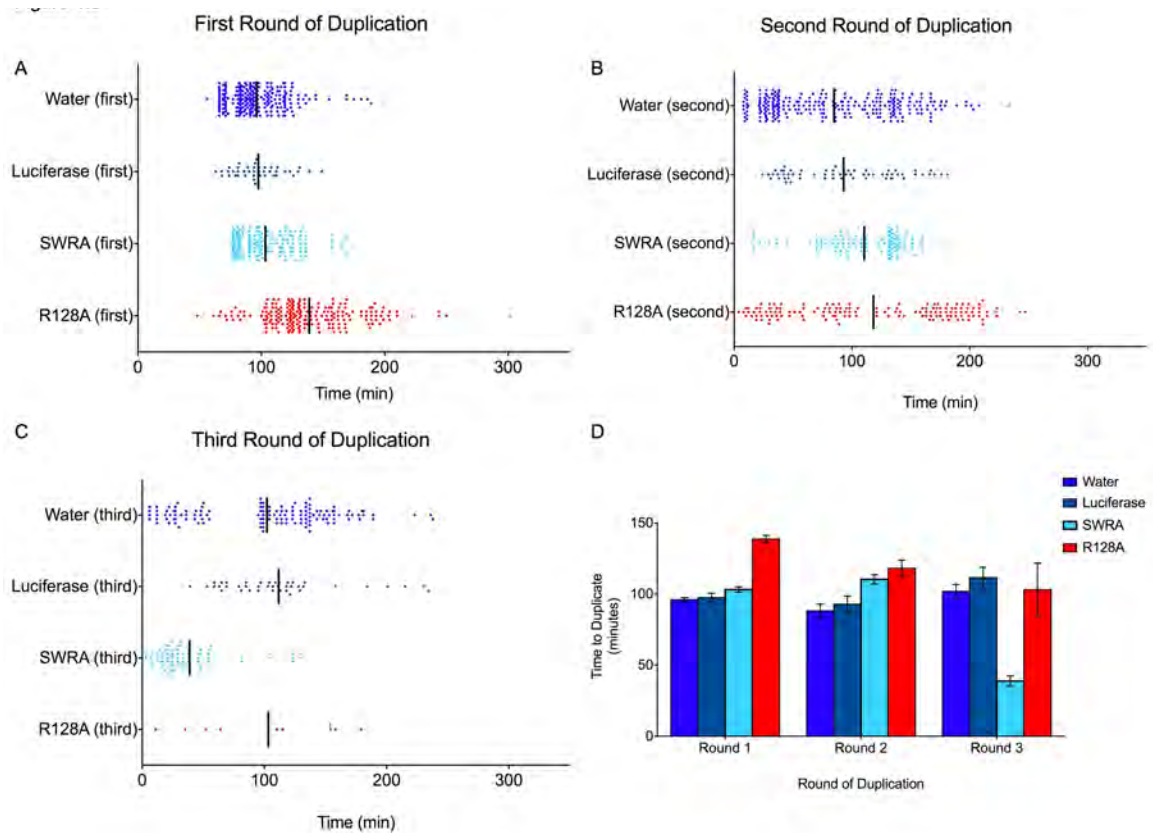


Figure 4.5 – The timing of centrosome duplication events. (A-C) Each dot represents a single centrosome duplication event at each round. The vertical lines amidst the dots show the mean doubling time. Times are minutes from the start of the filming or from the previous round of doubling (A) Represents the first duplication, (B) is the second, and (C) is the third. (D) Average time to double (+/- SEM) for all conditions at all rounds.

Average Time Between Each Round of Centrosome Duplication

Condition Tested	Round 1	Round 2	Round 3
R128A	138.8 +/- 2.5 N=211	118.2 +/- 5.8 N=145	103.2 +/- 19 N=10
Water	96 +/- 1.4 N=250	88.2 +/- 4.7 N=272	102.0 +/- 4.9 N=131
Luciferase	97.5 +/- 3.1 N=42	92.9 +/- 5.8 N=61	111.7 +/- 7.3 N=41
SW/RA	103.3 +/- 2.3 N=161	110.4 +/- 3.3 N=132	38.8 +/- 3.7 N=71

Table 4.2 – Comparison of Average Centrosome Duplication Times. The average time between centrosome duplication events was calculated for each condition tested and reported as mean +/- SEM. Round 1 is the average time from the beginning of the experiment to the first centrosome duplication.

pronounced in the first duplication than in subsequent duplications (Figure 4.5.A versus B and C).

Cyclin E mutant forms at the centrosome.

We characterized the centrosomal localization of our GFP-tagged cyclin E mutants in *Xenopus* extract and *Xenopus* S3 cultured cells to address the question of whether the translated mutant proteins were localizing to the centrosome and displacing endogenous cyclin E.

Aliquots of *Xenopus* extracts expressing GFP-tagged mutant cyclin E proteins were observed using widefield-fluorescence microscopy. The fluorescence signal was amplified using Alexa Fluor 488 conjugated rabbit anti-GFP antibody. Although background fluorescence was very high, GFP was seen in nuclei as expected (Ohtsubo et al., 1995) (Figure 4.6.A-F). Centrosomes were located using X-rhodamine tubulin to label microtubule asters nucleated by the centrosomes. We observed diffuse GFP and Alexa Fluor 488 anti-GFP signal throughout the cytoplasm but no specific concentration at the centrosome (Figure 4.6.G-I).

GFP-tagged R128A cyclin E was transfected into *Xenopus* S3 cells and observed by fluorescence microscopy 24-48 hours later to determine whether the protein localized to the centrosome as previously reported for CHO cells (Matsumoto and Maller, 2004; Ferguson and Maller, 2010; Ferguson and Maller, 2008; Ferguson et al., 2010). Although transfection efficiency was low (less than 1%), the cells that clearly expressed GFP in the nucleus were imaged to look for

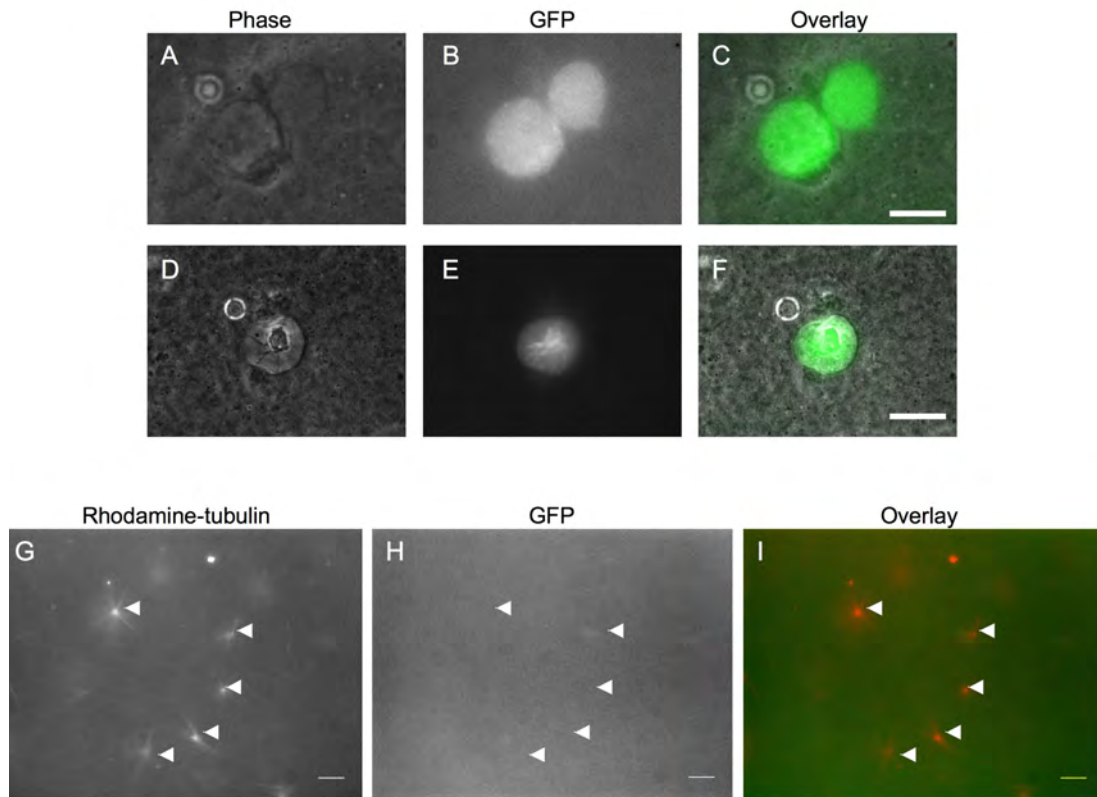


Figure 4.6 – Localization of GFP-cyclin E in *Xenopus* extracts. Polyclonal anti-GFP antibodies, directly conjugated to Alexa Fluor 488, were added to extract at a final dilution of 1:400 and observed using phase/fluorescence imaging. Panels A-C show the localization of R128A-GFP for two adjacent nuclei. Panels D-F show the localization of R128A-GFP for another nucleus in a separate experiment. Images in Panels A-F were taken with a 63x 1.32NA objective. Scale bars for A-F are 10 μ m. To visualize centrosomes, X-rhodamine conjugated tubulin was added to *Xenopus* extract to a final concentration of 10 μ g/ml to mark microtubule asters. Panel G shows several microtubule asters marked with X-rhodamine tubulin. Panel H shows the localization of GFP and anti-GFP-Alexa Fluor 488. Panel I shows an overlay of G and H. Aster centers (centrosomes) are marked with arrowheads in G-I. Images in Panels G-I were taken with a 20x 0.4NA objective. Scale bars for G-I are 100 μ m.

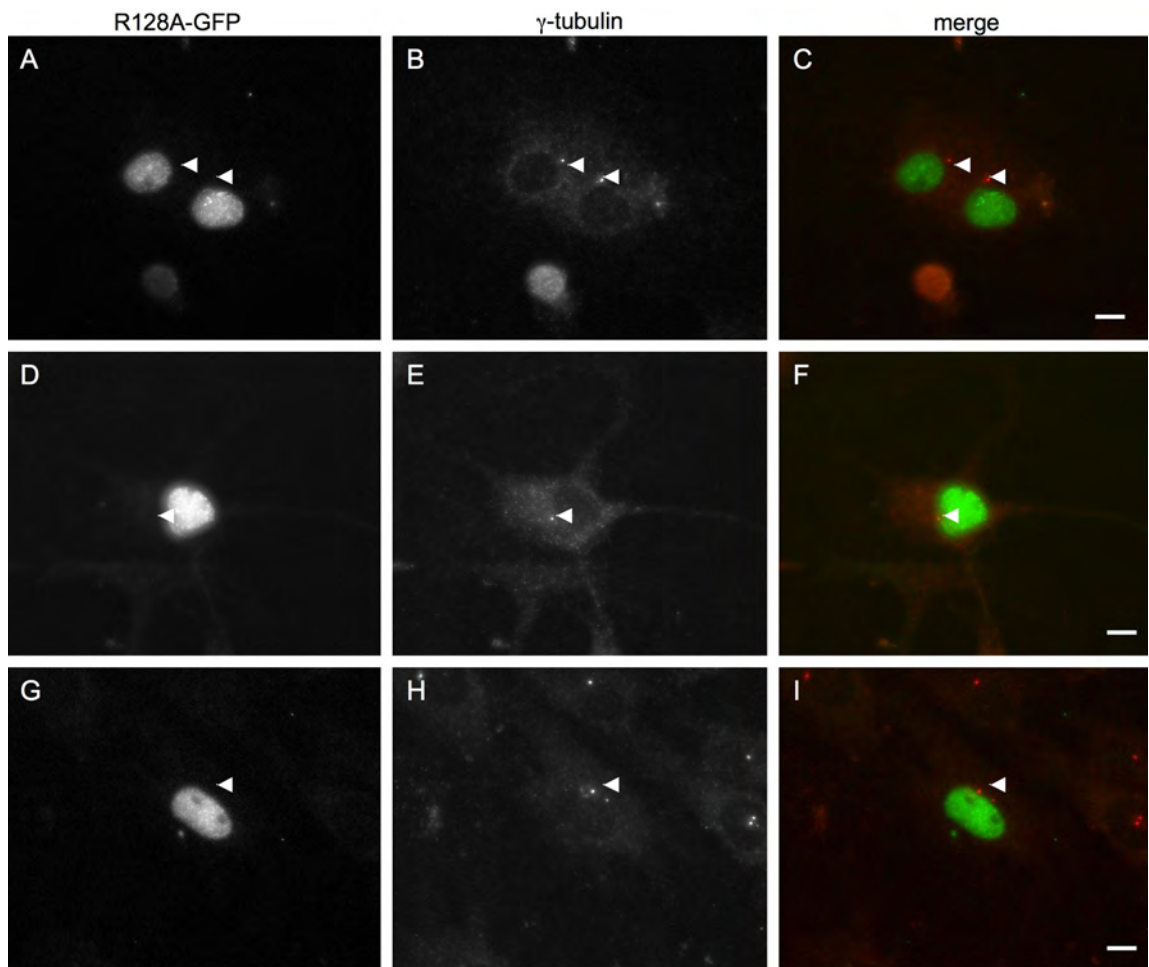


Figure 4.7 – Localization of GFP-cyclin E in *Xenopus* S3 cells. An R128A containing expression vector, driven by CMV promoter, was transfected into cells and observed 24 hours later. The left column (A, D, and G) shows the GFP localization in four different cells. The middle column (B, E, and H) shows the γ -tubulin localization. Overlays of GFP and γ -tubulin signals are shown in C, F, and I. Scale bars are 10 μ m. Locations of γ -tubulin concentrations (centrosomes) are marked with arrowheads.

centrosomal localization. Following live-cell analysis, cells were fixed and labeled for γ -tubulin (to mark centrosomes). Figure 4.7 shows the pattern of GFP label compared to the γ -tubulin localization within the S3 cells.

Discussion

We were intrigued by the discovery of a centrosome localization sequence in cyclin E (Matsumoto and Maller, 2004), a protein known to play a role in centrosome duplication (Matsumoto et al., 1999; Hinchcliffe et al., 1999; Lacey et al., 1999). The observations that the CLS plays a role in promoting S-phase entry and DNA synthesis (Matsumoto and Maller, 2004; Ferguson and Maller, 2010) prompted us to ask the question of whether it is also important for promoting centrosome duplication. In addition, we addressed the question of whether cyclin E alone at the centrosome is sufficient to promote duplication, as described for S-phase entry (Matsumoto and Maller, 2004) or if it must be in complex with CDK2.

Centrosome Duplication Dynamics in the presence of R128A

When we express the CDK2-binding deficient cyclin E mutant (R128A) in cycling *Xenopus* extract we see a clear reduction in the percentage of centrosomes that duplicate from round to round (Figure 4.3), a significant increase in the amount of time it takes for duplication to occur (Figure 4.5.A; Table 4.2) and an overall decrease in the average number of centrosome duplication cycles (Figure 4.4; Table 4.1) compared to controls. We do not see these same effects on centrosome duplication in extracts expressing the double mutant cyclin E that also lacks the CLS (SW/RA). We therefore conclude that

R128A is acting in a dominant-negative fashion to displace endogenous cyclin E from the centrosome as reported for CHO cells (Matsumoto and Maller, 2004). We believe this has the effect of lowering the local concentration of active CDK2/cyclin E and thus blocking the kinase activity from promoting centrosome duplication.

We did not observe a 100% block to centrosome duplication in the presence of R128A. This is likely due to the fact that we did not deplete any endogenous proteins; there is still WT cyclin E present in the extract. The mutant is thus acting as a competitive inhibitor of duplication in a background of normal WT cyclin E. It's possible that the amount of mutant protein available to displace endogenous cyclin E from its targets is limiting. The expressed protein levels stay relatively high throughout the 6 hour experiment (Figure 4.2.B), so a possible explanation is that all of the translated exogenous R128A protein is bound to its targets and that the centrosomes that are still duplicating the third time (roughly 2% of the input centrosomes) simply do not have mutant cyclin E present to displace the endogenous.

Cyclin E localization at the Centrosome

Considering previous cyclin E localization results (Matsumoto and Maller, 2004; Ferguson and Maller, 2010; Ferguson et al., 2010; Ferguson and Maller, 2008), it was reasonable for us to predict that this CLS-dependent action was taking place at the centrosome. The lack of visible cyclin E at the centrosomes in

our experimental systems doesn't necessarily mean there isn't any present. The results previously reported clearly show a concentration of cyclin E at centrosomes that is dependent on a functional CLS. In addition, they show the displacement of endogenous cyclin E in the presence of a GFP-CLS fragment (Matsumoto and Maller, 2004; Ferguson and Maller, 2010). Our results demonstrate a phenotype that is consistent with a CLS-dependent centrosomal function of CDK2.

It is possible that the amount of mutant cyclin E required to localize at the centrosome to block centrosome duplication is very small and is not enough to provide us with an adequate signal to detect by fluorescence microscopy. In the live extract system, the high level of background makes finding even a moderate increase in concentration difficult to observe. This is especially true given the fact that we sought to over-express the mutant protein in order to out-compete the endogenous WT cyclin E. This also holds true for our transfected S3 cells.

Centrosome duplication depends on CDK2 at the Centrosome

Our results indicate that CDK2 must be in complex with cyclin E at the centrosome in order to promote centrosome duplication. The dominant-negative effect that R128A has on centrosome duplication indicates that cyclin E is present at its CLS-directed target, but that cyclin E is not sufficient to promote the duplication process. This is the first demonstration of a separation of function for cyclin E in cell cycle control versus centrosome duplication control. Endogenous

WT cyclin E and CDK2 should still be in complex with each other in the cytoplasm. However, we believe the CDK2 activities are displaced from the centrosome by the presence of R128A. Thus, the cytoplasmic pool of active CDK2 is not sufficient to promote centrosome duplication.

Centrosome Duplication and the CLS

Our results point to a possible mechanism that imparts an additional layer of centrosome duplication control beyond simply regulating the total soluble cellular pool of CDK2/cyclin E. By controlling the localization of CDK2 to its target, the cell could regulate kinase activity to sub-cellular compartments without having to lower the overall cellular protein expression level. A cell in S-phase maintains a high level of CDK2 activity to simultaneously promote S-phase specific activities (i.e. DNA duplication) while suppressing late G1 activities (i.e. loading of DNA replication factors). Regulating a centrosomally localized pool of CDK2 would allow the cell to protect centrosomes from this high global activity when centrosome duplication promoting activity is no longer necessary; and might prove to be detrimental.

A particularly interesting demonstration of centrosome duplication regulation in the face of constitutively high expression of cyclin E in conjunction with known high levels of CDK2 activity is seen in the developing embryos of *Xenopus* (Hartley et al., 1996; Rempel et al., 1995) and sea urchins (Schnackenberg et al., 2008; Sumerel et al., 2001; Hinchcliffe et al., 1998).

Centrosome duplication is highly regulated in these systems even though the cyclin E protein level does not oscillate and the kinase activity remains high. Our results provide an explanation of how centrosome duplication could be regulated locally while soluble cytoplasmic pools of active kinase are still active.

Future Directions

Biochemical Interactions of Cyclin E Mutants

In order to abolish CDK2 binding of *Xenopus* cyclin E, R128 was mutated to alanine. This site corresponds with R131 in rat cyclin E, a site required for CDK2 binding as previously reported (Matsumoto and Maller, 2004). Mutation of T178 in *Xenopus*, corresponding with S180 in rat, did not exhibit as complete a lack of kinase activity as seen with R128A (personal communication, Frank Eckerdt). Thus, the R128A mutant was chosen as the CDK2 binding deficient mutant to test instead of the T178A which would have more closely resembled the previously reported cyclin E mutant.

Although a kinase assay was performed to compare R128A with T178A, and to validate that R128A had no kinase activity, these assays were performed using purified proteins expressed from baculovirus (data not shown, personal communication, Frank Eckerdt). To confirm that this behavior is consistent in *Xenopus* extract, an immunoprecipitation with anti-GFP followed by a probe with anti-CDK2 antibody should be done to demonstrate a lack of CDK2 binding specifically in the extract system. Any immunoprecipitated complex, or lack thereof, should be subjected to a histone H1 kinase assay to confirm a lack of kinase activity. This should be compared with the kinase activity of GFP-tagged WT cyclin E.

We expect that endogenous kinase activity is not disturbed in extract in which cyclin E is displaced from the centrosome. However, this should be confirmed with a kinase assay performed on endogenous CDK2 complexes immunoprecipitated with anti CDK2 antibody in the presence of the R128A mutant. Alternatively, immunoprecipitation using a cyclin E antibody could be done in the presence of a GFP-tagged CLS fragment. The CLS fragment should displace endogenous cyclin E from the centrosome as previously reported (Matsumoto and Maller, 2004).

Disruption of CDK2 Activity at the Centrosome

Demonstrating the localization of the R128A mutant cyclin E to the centrosome, and/or the displacement of endogenous cyclin E/CDK2 from the centrosome, is of critical importance to this study. There are several possible methods that should all be investigated together to clearly demonstrate the mechanism of action that results in the obvious phenotype reported.

We attempted to visualize the localization of GFP-tagged cyclin E mutants in live *Xenopus* extract with no success. A better approach would be to centrifuge the microtubule asters out of the extract onto a coverslip and label with anti-GFP and anti- γ -tubulin antibodies (Evans et al., 1985). This would eliminate the high background fluorescence of GFP and provide clear evidence of a strong binding of the mutant to the centrosome. We would expect to see co-localization of GFP-tagged WT cyclin E with the γ -tubulin signal, but not R128A or SW/RA.

In addition to demonstrating the localization of our mutant cyclin E variants to the centrosome, it would be important to demonstrate the displacement of endogenous cyclin E from the centrosome. Distinguishing between endogenous cyclin E and GFP-tagged mutant cyclin E expressed from our mRNA is not possible by simply using an antibody against cyclin E in an immunofluorescence application. However, expression of a GFP-tagged CLS peptide fragment would allow us to visualize endogenous cyclin E separately from the CLS peptide. GFP-CLS would not work for our centrosome duplication assay because it blocks S-phase entry (Matsumoto and Maller, 2004; Ferguson and Maller, 2010). However, it would be essential to use for testing localization.

In order to perform any studies on the localization of endogenous cyclin E, we would have to make our own antibody to *Xenopus* cyclin E because none of the antibodies that we used were able to detect any forms of cyclin E in our experiments. We would be certain to design the antibody to not recognize the CLS peptide fragment.

While knowing the localization of the cyclin E proteins relative to the centrosome is critical, it would also be important to demonstrate a difference in CDK2 localization and activity in the presence of the mutant forms of cyclin E. The same assay of centrifuging the asters out of the extract should be performed using anti CDK2 antibodies to see if endogenous CDK2 is displaced from the centrosome.

To demonstrate a difference in kinase activity between the centrosome and the rest of the cytoplasm, we could conduct a kinase assay on a centrosome containing fraction of extract and compare that to the cytoplasmic fraction in the presence of GFP-tagged R128A versus WT cyclin E. This would clarify whether there was a difference in the localized CDK2 activity at the centrosome in the presence of the mutant cyclin E.

Additional Control Conditions

Additional controls should be performed to clarify the effect of R128A expression on centrosome duplication. Expression of a GFP-tagged WT cyclin E should bind to the centrosome and should be able to form a complex with CDK2. Over-expression of cyclin E can be toxic to cultured CHO-K1 cells through an unknown mechanism (personal communication, James Maller). Binding of excess cyclin E to CDK2 may also increase overall kinase activity within the extract. However, it is not expected that there would be any effect on centrosome duplication.

The cell cycle state of the extract should be assayed in the presence of each mutant and the WT. Using BrdU added at several different times, we can determine whether the cycling extract, without Aphidicolin added, is able to repeatedly enter S-phase and replicate DNA in the presence of each mutant. As a control, expression of a GFP-tagged CLS fragment should block S-phase entry as previously reported (Matsumoto and Maller, 2004). We expect that the extract

will be able to enter S-phase in the presence of R128A, SW/RA, and the WT based on earlier findings (Matsumoto and Maller, 2004).

Confirmation of Phenotype in Additional Systems:

Many of the controls to be performed in *Xenopus* have already been reported in a CHO-K1 cell line (Matsumoto and Maller, 2004). This also includes a clear demonstration of both the localization of the mutants to the centrosome as well as the displacement of endogenous cyclin E from the centrosome. The study of centrosome duplication in this system has not been conducted, however, and this system would provide a way to confirm that the results reported here are not specific to an embryonic system.

CHO-K1 cells exhibit multiple rounds of centrosome duplication when arrested in S-phase (Balczon et al., 1995). Assaying for centrosome duplication could be conducted using established cell lines that have inducible expression of myc-tagged cyclin E mutants (personal communication, Rebecca Ferguson). Centrosome number could be determined by fixation of the cells and staining for centrosomes using anti- γ -tubulin antibodies, or anti-centrin antibodies following induction of protein expression and S-phase arrest of different durations (36, 48 and 72 hours).

Taken together, the above experiments would confirm that the block to centrosome duplication that was demonstrated in the *Xenopus* extract is due to the disruption of a specific kinase event localized to the centrosome.

Materials and Methods

All chemicals were obtained from Sigma-Aldrich (St. Louis, MO) unless otherwise stated.

***Xenopus laevis* cytoplasmic extract**

Xenopus extract was prepared using a modified protocol based on a previously published report (Hinchcliffe and Sluder, 2001). For a detailed description of the preparation of *Xenopus* extract, please refer to Appendix A. Briefly, eggs from *Xenopus laevis* frogs were collected from hormone-injected females, washed, and crushed by centrifugation to generate a cell-free cytoplasmic extract. Cytochalasin-D, protease inhibitors, and an ATP-containing energy mix were all added to the extract prior to the addition of centrosomes. Demembrated *Xenopus* sperm heads were added to provide a source of centrioles and DNA. Aphidicolin was added to block DNA synthesis and permanently lock extracts in S-phase.

Image Collection and Analysis

Microtubule asters were visualized using modified Zeiss ACM polarized light microscopes. Images were captured using either a Hamamatsu C2400 camera through an Argus 20 Image Processor (Hamamatsu Corp., Bridgewater, NJ), or a Q-Imaging Retiga 1300 (Photometrics, Tucson, AZ). Digital images were recorded using either Adobe Premiere 5.1 (Adobe Systems, Inc, San Jose, CA) or Simple PCI 6.0 (Hamamatsu Corp., Bridgewater, NJ). Images were

acquired every 20 seconds and assembled into time-lapse movies using Quicktime 7.2 (Apple, Inc, Cupertino, CA).

Multimode images (phase/fluorescence) were acquired with a Q-Imaging Retiga EXi camera (Photometrics, Tucson, AZ) on a Leica DMRXE microscope (Leica Microsystems, Buffalo Grove, IL) using either a 20x 0.4NA Plan Fluotar air objective or a 63x 1.32NA Plan Achromat oil-immersion objective. Images were digitally acquired and stored using Slidebook 5.0 (Intelligent Imaging Innovations, Denver, CO). Final images were adjusted for display using ImageJ.

We followed individual asters over time and counted each time that a single aster split into two. To determine the percentage of asters that duplicated at the first round, we took the ratio of asters that duplicated to the number of asters that were present in the field of view to begin. To determine the percentage of asters that duplicated in each subsequent round, we took the ratio of asters that duplicated to the total number of asters that resulted from the previous round of duplication. The time from the start of the experiment to each duplication was also recorded and used to determine the average time to duplicate at each round. To obtain “average number of duplications” we followed the lineage of every aster that was present at the end of the data set. We counted backwards from the end of the movie to determine the number of doublings that the final aster underwent during the course of the experiment. For a schematic of how centrosome duplication was analyzed, please refer to Figure 4.1.D.

Creation of Cyclin E Mutants

Mutant forms of *Xenopus laevis* cyclin E, in pBAC-2cp, were obtained from the lab of James Maller, HHMI at the University of Colorado Medical School (Denver, CO). Mutations of the original coding sequence were made in the Maller lab using the QuikChange system (Agilent Technologies, Santa Clara, CA). The centrosome localization signal (CLS) in rat cyclin E was disrupted by mutation of four key residues, S234, W235, N237 and Q241, to alanine. This mutation abolished cyclin E co-localization with γ -tubulin (Matsumoto and Maller, 2004). The corresponding residues, S247, W248, N250 and Q254, in *Xenopus* cyclin E were mutated to alanine to generate the SWNQ-(A) mutant. Residue S180 in rat cyclin E is required for CDK2 binding as mutation to aspartic acid abolished any association with CDK2 (Matsumoto and Maller, 2004). The corresponding amino acid was mapped to R128 in *Xenopus* cyclin E and was mutated to alanine to create the mutant R128A. In addition, a third mutant was created that was the combination of the CLS mutant and the CDK2 binding mutant – referred to a SW/RA.

Creation of Cyclin E-GFP Fusion Proteins

Mutant cyclin-E coding sequences were cloned out of the original pBAC-2cp vector using PCR. The following primer sequences were used:

Forward: 5'-CACCATGCCAGTGATAAGC-3'

Reverse: 5'-CGGCTTGTCTGCTCGAT-3'

Phusion High Fidelity DNA polymerase (Finnzymes, Inc, Woburn, MA) was used for PCR following the manufacturer's instructions.

The PCR product was cloned into the Gateway® -compatible vector pENTR/D-TOPO (Invitrogen, Carlsbad, CA) according to the manufacturer's instructions. The sequence was then transferred, using a standard Gateway® L-R Clonase reaction into pcDNA-DEST47 (Invitrogen) to create a C-terminal GFP fusion of each mutant. The final vector contains both a T7 promoter for creation of mRNA (see below) and a CMV promoter for expression in tissue culture cells.

Sequence integrity was verified using standard Sanger DNA Sequencing performed by Genewiz (South Plainfield, NJ). Sequence alignment was verified using MacVector (MacVector, Inc, Cary, NC).

Messenger RNA Generation

Messenger RNA was generated using mMessage mMachine® T7 Ultra from Ambion (#AM1345, Applied Biosystems, Foster City, CA). Final mRNA product was recovered by phenol:chloroform extraction followed by isopropanol precipitation and resuspended in nuclease-free water to a final concentration of 1mg/ml.

Integrity of mRNA was confirmed for each generated batch using ethidium bromide agarose gel electrophoresis. In addition, to confirm that mRNA was functional for translation, *in vitro* translation of synthesized mRNA was carried out

using a nuclease-treated rabbit reticulocyte lysate (#L4690, Promega Corporation, Madison, WI). Protein was translated in the presence of Transcend™ tRNA to incorporate biotinylated lysine residues for colorimetric detection via Streptavidin-AP conjugates (#L5070, Promega). Validated mRNA was stored at -80°C in 5µl aliquots.

Use of mRNA in *Xenopus* extracts

For each experiment, 150µl of extract containing protease inhibitors, cytochalasin-D and Aphidicolin was prepared for centrosome duplication. Sperm nuclei (1:100) and energy mix (1:40) were added and the extract was split into 3 x 50µl sample tubes. To each tube, 1µl of 1mg/ml mRNA of each mutant being tested was added – final concentration 20ng/µl. To control for the effects of dilution, one preparation was always made with 1µl of nuclease-free water.

Protein Expression and Detection

Samples of extract were taken at specified times to assay for mutant protein expression. Samples in 1x SDS loading buffer were denatured at 95°C for 10 minutes and either used immediately or stored at -80°C. Frozen samples were re-denatured prior to PAGE. Proteins (15-30µg total/well) were separated on 12% tris-glycine acrylamide gels (120V constant voltage for 60-90 minutes). Proteins were transferred to nitrocellulose membranes overnight at 4°C at 90mA constant current.

Mutant fusion proteins were detected with mouse anti-GFP antibodies (1:500) (Clone B-2, #sc-9996, Santa Cruz, CA). Secondary horseradish peroxidase-conjugated antibodies were used (1:10,000) for detection via enhanced chemiluminescence (SuperSignal West Pico Chemiluminescent Substrate, 34080, Thermo Scientific, Rockford, IL).

Cell Culture and Transfection

Xenopus S3 cells were a generous gift from the lab of P. Todd Stukenberg (University of Virginia). Cells were grown in 75% L-15, 15% distilled water, 20% Fetal Bovine Serum (Invitrogen, Carlsbad, CA) at 25°C in a dark, non-humidified chamber. Transfections were carried out with either FuGENE (Roche, Madison, WI), Lipofectamine LTX (Invitrogen, Carlsbad, CA), or PolyJet (Signagen Laboratories, Rockville, MD) using the manufacturer's instructions.

Immunofluorescence

Standard Protocol

Cells were grown on 22mm square #1.5 coverslips in 6-well dishes. Coverslips were fixed in -20°C methanol for 5-10 minutes. The cells were then rehydrated for 5 minutes in PBS followed by 1 hour at 37°C in blocking buffer (PBS, 1%BSA, 0.5% Tween-20). Antibody incubations were carried out at 37°C for 1 hour (primary) and 30 minutes (secondary). Between antibody incubations, cells were washed 3 x 5 minutes in PBS, 0.5% Tween-20. Coverslips were given

a final wash for 5 minutes in PBS and then briefly immersed in distilled water before being mounted on a 7 μ l drop of 1:1 PBS:glycerol mounting media.

Coverslips were sealed to slides with quick-drying clear nail polish.

Antibodies used:

The following primary antibodies were used at the following dilutions of stock where indicated in the Results section:

Santa Cruz Biotechnology (Santa Cruz, CA)

Anti GFP (mouse B-2): SC-9996 (1:100)

Invitrogen (Carlsbad, CA)

Alexa Fluor 488 Anti-GFP (rabbit): A21311 (1:400)

Sigma (St. Louis, MO)

Anti γ -tubulin (mouse GTU88): T6557 (1:500)

Anti γ -tubulin (rabbit): T5192 (1:1000)

Anti α -tubulin (mouse B-5-1-2): T6074 (1:500)

The following secondary antibodies were used at the following dilutions of stock where indicated in the Results section:

Invitrogen (Carlsbad, CA)

Goat anti-mouse Alexa Fluor 488: A10680 (1:1000)

Goat anti-rabbit Alexa Fluor 594: A11012 (1:1000)

Thermo Scientific (Rockford, IL)

Goat anti-mouse HRP: 32430 (1:10,000)

Goat anti-rabbit HRP:32460 (1:10,000)

Chapter V

General Discussion

The work presented in this thesis cover three separate areas of study related to centrosomes and their duplication. Taken together, my work has made significant contributions to the understanding of the consequences of having multiple centrosomes (Chapter III), the cellular response to loss of the centrosomes (Appendix A), and the means of regulating the centrosome duplication process through sub-cellular regulation of kinase activity (Chapter IV). Several of the observations presented in this work have been confirmed and expanded upon by other researchers as outlined below. In addition, I have posed some questions that still remain that relate to this work.

Supernumary Centrosomes and Cell Proliferation

The proposed connection between loss of p53, multiple centrosomes, and cancer (Lingle et al., 1998; Lingle et al., 2002; Pihan et al., 1998; Pihan et al., 2001; Pihan et al., 2003; Fukasawa et al., 1996; Tarapore and Fukasawa, 2002) (reviewed in: D'assoro et al., 2002; Fukasawa, 2007) was intriguing to us, but posed a conundrum. We wanted to know how cells with multiple centrosomes, presumed to undergo multipolar divisions and induce gross chromosome segregation errors, could continue to propagate? We investigated this question by characterizing the mitosis of multiple generations of p53-null mouse embryonic fibroblasts.

Our findings demonstrated that a population of cells, almost 40% of which have supernumary centrosomes, are able to complete mostly normal bipolar

divisions greater than 90% of the time (Figure 3.2). Our characterization of those cells during mitosis indicated that the extra centrosomes are focused into two poles by anaphase (Figure 3.1). This provided an explanation of how cells are able to cope with multiple centrosomes and still proliferate. It was our ability to conduct long-term, live-cell imaging experiments that ultimately provided the first real insight into how cells with multiple centrosomes could continue to survive and contribute to tumorigenesis.

The mechanism for spindle pole bundling has been explored further and our initial findings have been confirmed and expanded upon. It has been shown that the spindle pole bundling is dependent on NuMA, HSET, and dynein (Quintyne et al., 2005; Kwon et al., 2008). And further work on investigating the mechanics of multipolar divisions has revealed that gross multipolar divisions actually produce non-viable cells. However, the presence of multiple centrosomes contributes significantly to chromosomal instability through the formation of merotelic attachments of chromosomes to the spindle while the cell is in the act of bundling the extra spindle poles (Ganem et al., 2009). Thus, extra centrosomes do contribute to genomic instability, although not through the mechanisms previously thought, i.e., the segregation of genetic material to more than two daughters.

Still open for debate is the question of whether or not centrosome amplification is a cause or a consequence of cancer in a p53-null background. Does the loss of p53 directly result in a deregulation of the normal centrosome

duplication cycle? Does the centrosome duplicate twice, or are multiple daughters formed around a single mother centriole? Or does p53 loss lead to an increase in centrosome number through defects in cytokinesis? Using cell lines established from p53-null mice is problematic because the cell line is established from those cells that have increased survival characteristics and may not be truly representative of a cell immediately after loss of gene function. To address this question, one could generate a cell line from a normal human cell, such as the hTERT-RPE1, in which both alleles of p53 could be rendered null by homologous recombination somatic cell knockout as applied by Bert Vogelstein (Chan et al., 1999). This would allow for the direct assay of centrosome number following functional p53 elimination.

The Centrosome in Cell Cycle Progression:

The observation that centrosome loss induced a G1 arrest in the subsequent cell cycle (Hinchcliffe et al., 2001) prompted us to investigate the mechanism for the arrest. We sought to explore the putative centrosome checkpoint in a human cell line that had functional checkpoint proteins such as p53 and p21. Therefore, we conducted our microsurgical removal experiments in hTERT-RPE1 cells that stably express GFP-centrin1 to label centrioles. We found that these cells did not arrest in G1 as previously reported (Uetake et al., 2007).

We returned to the original cell line (BSC-1) used in the earlier study in an effort to repeat the reported results. We found that these cells also did not arrest in G1 (Figure A.3). We instead found that the arrest was dependent on additional cell stressors such as light used to image the cells, as well as micromanipulation methods and cell growth conditions in our viewing chambers (Figure A.1).

This study contributed to the growing body of knowledge that the centrosome is not simply a follower of the cell cycle, but in fact plays an important role in cell cycle progression. Although the cell does not directly monitor for the presence of a centrosome to promote the G1-S phase transition, it is clear that the absence of a centrosome is considered a cellular stress that initiates a p38-dependent cell cycle arrest (Uetake et al., 2007).

My work within this study also addressed a concern that affects all research that employs live-cell imaging as a means to observe phenotypes. Extreme care must be taken to minimize photo-damage induced by the observation conditions. It is imperative that the researcher controls for the possible impact of the observation conditions, in addition to the experimental manipulations, to avoid drawing improper conclusions from phenotypes such as cell cycle arrest. Our observations have implications in the interpretation of other studies that suggest centrosome damage was the sole cause of G1 arrest (Mikule et al., 2007) when the RNAi used to induce the damage may have been a source of additional stress.

CDK2, Cyclin E, and Centrosome Duplication

We tested whether centrosomal localization of CDK2/cyclin E was necessary to promote centrosome duplication using *Xenopus* egg extracts. Although it was well known that CDK2 kinase activity was required for both S-phase entry and centrosome duplication, (Hinchcliffe et al., 1999; Lacey et al., 1999; Krude et al., 1997; Takisawa et al., 2000), prior to our observations, there was no indication that there was a functional difference between CDK2/cyclin E activity to promote S-phase entry and for centrosome duplication.

Our finding that cyclin E localization via a centrosome localization signal (CLS) was not sufficient to promote centrosome duplication (Figures 4.3, 4.4, and 4.5) presented an interesting contrast to the findings that the CLS-mediated binding of cyclin E to the centrosome was necessary and sufficient to promote S-phase entry (Matsumoto and Maller, 2004). This was the first indication of a separation of functions of cyclin E between centrosome duplication and cell cycle progression.

We looked for the concentration of cyclin E at the centrosomes in our *Xenopus* extract as well as in transfected *Xenopus* S3 cells and were unable to see any specific locally increased amounts (Figures 4.6 and 4.7). However, this does not mean that the protein was not present to affect a change in local kinase activity. We used GFP to tag the exogenously expressed mutant cyclin E protein. Cyclin E is present throughout the cytoplasm and thus created a large

GFP background signal. In S3 cultured *Xenopus* cells, we also did not see a centrosomal concentration of expressed mutant cyclin E. We had difficulty transfecting these cells and were left with a small population (less than 1%) to observe. It is possible that the mutant cyclin E localization required to disrupt native protein levels and block centrosome duplication is very transient and thus a low-frequency event in freely cycling cells.

A final consideration is the possibility that the action is not solely at the centrosome. The CLS does not only have to be a centrosome localization signal as it is so named. Our data supports the hypothesis that there is a CLS-dependent CDK2/cyclin E interaction that is required for centrosome duplication. We know that the CLS is also a substrate recognition domain for MCM5 (Ferguson and Maller, 2008). It is attractive to imagine that the targets for centrosome duplication would be located at the centrosome, but this is not the only possibility.

To strengthen our observations, we would like to see the dynamics of WT cyclin E localization at the centrosome as it functions in both normal duplication and during S-phase arrest. Observations of the cell-cycle dependent localization of a GFP-tagged WT cyclin E protein would provide insight into the normal dynamics of the protein's localization throughout the cell cycle. The R128A mutant form may not be regulated in the same way if CDK2 binding plays any role in directing the localization.

We also would like to see the displacement of endogenous cyclin E from the centrosome by the localization of the mutant as previously reported (Matsumoto and Maller, 2004). This would confirm our phenotype data that suggests that R128A is acting in a dominant negative fashion. If this experiment could be conducted in *Xenopus* extract, it could address the question of whether or not the centrosomes that continue to duplicate even in the presence of R128A are associated with WT or mutant forms of the protein.

The separation of function of cyclin E in promoting S-phase versus centrosome duplication that we report here is important when one considers that CDK2/cyclin E levels are maintained at a high level throughout all of S-phase, creating conditions permissible for centrosome duplication that persist for an extended time. Although there is a well-described block to reduplication for centrosomes involving a physical association of mother and daughter centrioles (Tsou and Stearns, 2006; Wong and Stearns, 2003), the licensing pathway has not been fully described. The requirement for localizing CDK2/cyclin E to a centrosomal substrate provides a possible mechanism for regulating duplication by increasing the centrosomal concentration of active CDK2 to an area of interest only at specific times.

Future Directions

Because there have already been several follow-up studies conducted that relate to the already published studies from this thesis (Chapter III, and

Appendix A), I am dedicating this section to explore some possible follow up studies related to the CLS-mediated CDK2/cyclin E requirement for centrosome duplication.

The notion of local control of CDK2 activity is intriguing in the context of what we now know is the role of PCM in determining daughter centriole number. When the PCM component pericentrin is over-expressed in S-phase arrested CHO cells, multiple daughter centrioles can form during duplication (Loncarek et al., 2008). Could CLS-mediated localization of cyclin E play a role in the regulation of pericentrin concentration? The CLS is also a known substrate-binding domain that is required to localize MCM5 to centrosomes (Ferguson and Maller, 2008). Could it be that the CLS influences pericentrin localization in a similar way?

In addition, over-expression of Plk4 also causes centrosome over-duplication, specifically by inducing multiple daughter centrioles around a single mother (Kleylein-Sohn et al., 2007) and even promoting *de novo* centriole formation (Eckerdt et al., 2011). It is still unknown how Plk4 activity, in relation to centrosome duplication, is regulated. Plk4 is activated by phosphorylation by an upstream kinase and it is that activated form that is seen at the centrosome (Sillibourne et al., 2010). It is possible that CLS-mediated localization of CDK2/cyclin E to the centrosome directs the local activation of Plk4 to promote centrosome duplication.

Could extra CDK2/cyclin E alone at the centrosome induce the formation of extra centrosomes? By fusing cyclin E to the PACT domain, in experiments similar to those conducted to test the cyclin E effects on DNA replication (Ferguson and Maller, 2010), excess WT cyclin E could be targeted to the centrosome and duplication could be assayed in either normal cycling cells or in S-phase arrested cells.

It would be interesting to know if local CDK2 activity plays a role in controlling the centrosomal localization of pericentrin, or if CDK2 is an upstream regulator of Plk4, specifically at the centrosome. An increase in centrosome duplication induced by providing an excess of centrosomally localized CDK2/cyclin E would indicate that regulating the localization, possibly through modification of the CLS, would be a critical step in blocking reduplication.

One question that clearly remains is how the CLS might itself be regulated to prevent cyclin E from being localized to the centrosome when it should be kept away. Mutation of the SWNQ residues to alanine completely abolished centrosomal localization (Matsumoto and Maller, 2004). This raises the question of whether those residues could be modified in a regulated way to block their function in a cell-cycle dependent way.

Understanding the centrosome is crucial to our understanding of the origin and propagation of cancer. By increasing our knowledge how centrosome defects

contribute to cancers, and how normal cells prevent those defects, one can hope to take advantage of the cells own control mechanisms for the development of new cancer therapies. The observations reported in this thesis have made a significant contribution to our understanding of the importance of the centrosome and its regulated duplication. Continued research in this field should lead to a clearer picture of the causes of, and cures for a devastating class of diseases.

Appendix A

Centrosome Loss is Functionally a Stress That Contributes to Cell Cycle Arrest

Abstract

The centrosome is the microtubule-organizing center of the cell. In mitosis, two centrosomes act in a dominant fashion to organize the mitotic spindle. The centrosome must be duplicated once and only once in each cell cycle. It has been reported that removal of the centrosome causes a G1 arrest in the next round of the cell cycle. We further investigated this phenomenon to determine what factors promoted this cell cycle arrest. We found that cells that had centrosomes microsurgically removed did not arrest in G1 as predictably as previously reported. Instead, the G1 arrest was dependent on additional stressors being put on the cell in addition to centrosome removal. The same stressors did not induce an arrest in cells that had a control microsurgical manipulation, or in cells in the same microscopic field of view. Our results suggest that the cell does not have a specific checkpoint that monitors for the presence of a centrosome in order to progress through the cell cycle. Instead, centrosome loss is a detectable stress that, when combined with additional stresses, leads to a G1 arrest.

Introduction

An interesting feature of the centrosome is that it is not always a passive organelle that simply follows the cell cycle; it also contributes to controlling cell cycle progression. It has been suggested that the centrosome acts as a scaffold for many enzymatic reactions for the cell (Rieder et al., 2001). Previous work has shown that cells without a centrosome were able to complete the cell cycle in which the centrosome was removed. However, in the subsequent cycle the cell would arrest in G1 (Hinchcliffe et al., 2001). A subsequent study showed that centrosome damage (from siRNA of centrosomal proteins) would also result in a similar G1 arrest that was dependent on p53 (Mikule et al., 2007). Taken together, these studies posed an interesting new paradigm in which the centrosome must be present and healthy in order to promote cell cycle progression. We investigated this phenomenon more closely and found a connection between the centrosome and stress detection and response.

Work in our lab, conducted by Yumi Uetake and Christopher English, revealed that in hTERT-RPE1 cells that had their centrosomes microsurgically removed, we no longer observed the G1 arrest previously reported in BSC-1 cells (Hinchcliffe et al., 2001). This was unexpected because the RPE-1 cell line was chosen for this study specifically because it has normal cell cycle checkpoints and should behave more like a normal cell than an immortalized or

transformed cell. We were certain that the centrosome had been removed because we were able to directly visualize centrioles that had been tagged with centrin1-GFP.

A close examination of our experimental parameters revealed to us that three components of our experimental workflow had changed since the original experiments were performed. The first change was that we were now using a more stable micromanipulator that provided us with more control during the microsurgery. The second change was that we were transferring coverslips from chambers that had an open side for manipulation to completely sealed chambers for observation. The previous study used the manipulation chambers for the duration of the experiment. The final change was that we began using digital cameras with much higher quantum-efficiency, which allowed us to use less incident light for our long-term observations.

These realizations prompted us to test the effects of modulating incident light on the cells in conjunction with centrosome removal, followed using either sealed or open chambers, to determine if these observational stressors act additively with centrosome removal to induce a G1 arrest.

Results

Hinchcliffe, et al. previously reported that after microsurgical removal of the centrosome during interphase, BSC-1 cells progressed through mitosis and 88% arrested in G1 after that mitosis (Hinchcliffe et al., 2001). To test how these previous results fit with our current findings that cells not only progress through the cell cycle, but form centrioles *de novo* (Uetake et al., 2007), we reinvestigated the consequences of microsurgical removal of the interphase centrosome from BSC-1 cells using our current methodology. Our current methods involve several system upgrades, such as the use of a mechanically more stable micromanipulator and more sensitive video cameras that allow ~64-fold lower green light (546 nm) intensities for time-lapse imaging (4.7 nW output from the condenser versus an estimated 302 nW condenser output previously used). Also, after microsurgery, we now remount the cell bearing coverslips into sealed observation chambers (Sluder et al., 2007) for time-lapse observations, rather than leaving them in oil-capped micromanipulation preparations. The sealed chambers contain an approximately three-fold higher volume of medium (600 μ l) (Figure A.1).

We cut a BSC-1 cell to remove the centrosome, and we performed a control amputation of cytoplasm from another cell in the same field of view. The untouched cells served as controls for incident light and media conditions. For some experiments, the coverslips were transferred after the microsurgery to

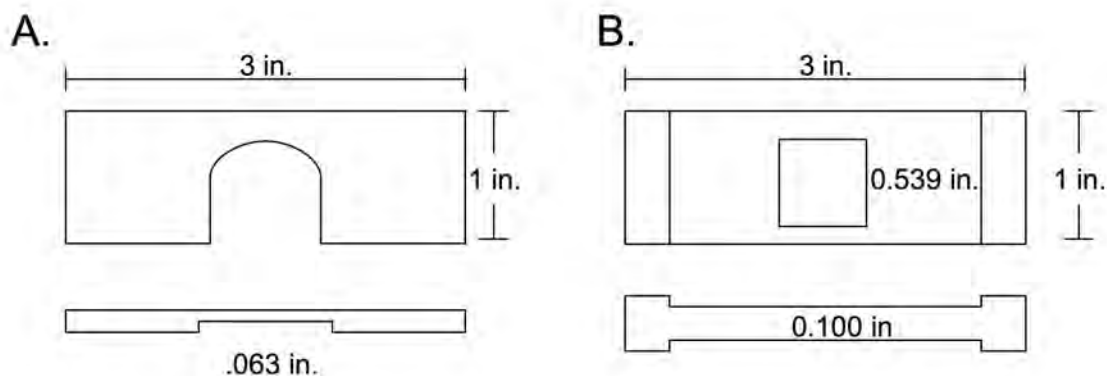
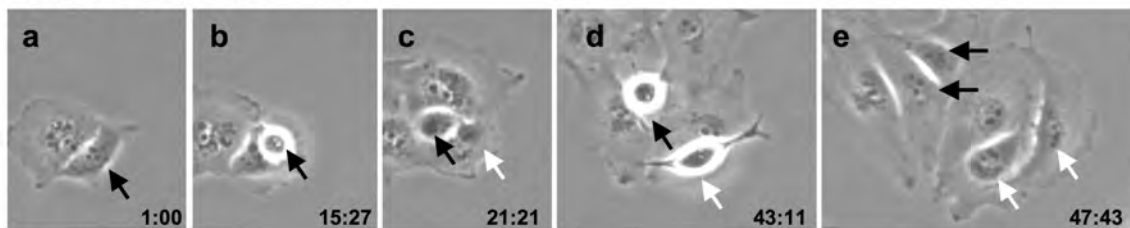


Figure A.1 – Cell manipulation and viewing chambers. (A) Diagram of an open-sided cell-micromanipulation chamber. Cells were grown on coverslips that were then mounted over the horseshoe shaped opening. Mineral oil was used to cap the open side of the chamber to allow for access by the glass microneedle. (B) Diagram of a sealed cell-viewing chamber. Coverslips were removed from the micromanipulation chamber and re-mounted on the viewing chamber. Here all sides are sealed and the volume of media is approximately 3 times greater than in the micromanipulation chamber (600 μ l versus 200 μ l).

sealed observation chambers (Figure A.1), as we have done after the microsurgery of RPE1 cells. For other experiments, we left the cells in the oil-capped micromanipulation preparations for time-lapse observations. Using our current, improved observation conditions, we found that only 14% of the acentrosomal cells arrested in interphase after mitosis, whereas none of the control amputation or untouched controls arrested in interphase (Figure A.2 and Figure A.3). When the cells were left in the micromanipulation chambers for time-lapse filming, 33% of the acentrosomal cells and 13% of the control-amputated cells arrested in interphase after mitosis; none of the untouched controls arrested (Figure A.3).

To test if acentrosomal BSC-1 cells are sensitive to the level of continuous green light used for time-lapse observations, we performed the same experiments, but raised the illumination intensity to 1,170-nW condenser output (3.8-fold higher than the Hinchcliffe et al. (2001) study). Our results (Figure A.3) show that for both the sealed and oil-capped micromanipulation chambers used for filming, a higher percentage of the acentrosomal cells (83%) and control cut cells (25%) arrest in interphase after mitosis under these higher green light conditions. Notably, none of the untouched control cells arrested under any of these conditions.

A - Low Light - Sealed Chamber



B - High Light - Manipulation Chamber

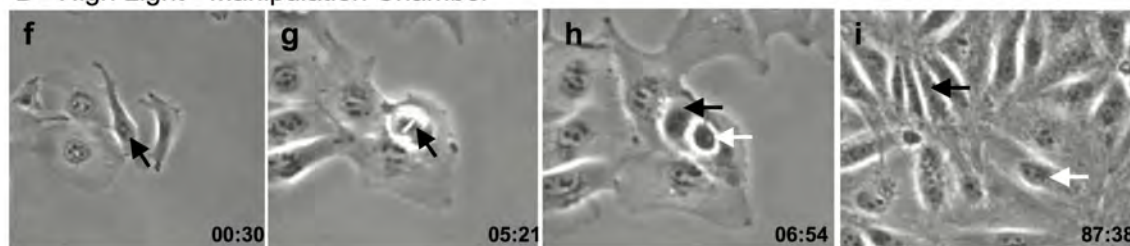


Figure A.2. – Cell Cycle Progression of BSC-1 Karyoplasts. (A) A BSC-1 karyoplast in a sealed cell-viewing chamber imaged with low light intensity. A karyoplast (a, black arrow) enters mitosis (b) and divides into two daughters 21-hours after microsurgery (c, black and white arrows). The daughters undergo another division approximately 22 hours later (d). (e) By 47 hours post microsurgery, the original karyoplast has divided twice (two black arrows and two white arrows). (B) A BSC-1 karyoplast in a micromanipulation chamber imaged with high light intensity. A karyoplast (f, black arrow) enters mitosis (g) 5 hours after microsurgery and divides into two daughters (h, black and white arrows). The daughter cells do not enter mitosis again even after 87 hours of observation (i, white and black arrows). Times are hh:mm.

Percent BSC-1 Cells Arresting in Interphase after Microsurgery

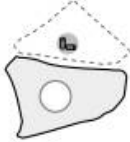
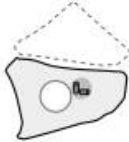

546nm green light intensity	Chamber type	Centrosome removal	Control amputation	Untouched control
				
Current	Sealed	14% (3/21)	0% (0/11)	0% (0/9)
	Oil capped	33% (3/9)	13% (1/8)	0% (0/9)
Higher	Sealed	25% (1/4)	22% (2/9)	0% (0/6)
	Oil capped	83% (10/12)	25% (2/8)	0% (0/9)

Figure A.3 - G1 progression of acentrosomal and control cut BSC-1 cells under various experimental conditions. For each experiment, an interphase cell was microsurgically cut to remove the centrosome and, in the same field, a cell was cut to amputate an equivalent portion of the cytoplasm without removing the centrosome. Untouched cells in the same field served as controls. After microsurgery in oil-capped micromanipulation chambers, cells were continuously cultured in the same chamber or transferred into a sealed filming chamber, and observed for 90h at the indicated intensity of 546-nm green light. After microsurgery, all cells went through mitosis, but thereafter some arrested in interphase. The “green light intensity” column indicates green light intensity used for time-lapse imaging. Current, 4.75 nW condenser output; Higher, 1170 nW condenser output. The “Chamber type” column indicates the chamber types used. Sealed, the sealed chamber currently used for time-lapse observation; Oil capped, the oil-capped chamber used for micromanipulation.

Discussion

To gain insight into the apparent difference between our present results and those of Hinchcliffe et al. (2001), we characterized the behavior of microsurgically produced BSC-1 acentrosomal cells and control-amputated cells using our current experimental conditions. Our observations reveal that acentrosomal BSC-1 cells behave in a qualitatively similar fashion to acentrosomal RPE1 and HMEC cells (Uetake et al., 2007). BSC-1 cells can progress through G1 without a centrosome under our current conditions, but not at as high a frequency as RPE1 cells.

Our observations indicate that G1 progression in BSC-1 cells may be more sensitive to the loss of the centrosome than in RPE1 cells, and micromanipulation chambers provide a less favorable environment than sealed chambers for the G1 progression of BSC-1 cells that have been stressed by microsurgery and loss of the centrosome. Also, the previous use of higher green light intensities for time-lapse observations than we currently use may have contributed to the previously reported G1 arrest of acentrosomal cells (Hinchcliffe et al., 2001).

Together, our results with human and BSC-1 cells reveal that the centrosome is not required for G1 progression in normal cells that have a

functional p53 pathway. This means that the centrosome and its activities are not an integral part of the mechanisms that drive the cell cycle through G1 into S phase. Our finding that interphase progression after centrosome removal occurred with normal kinetics indicates that the normal human cell does not have a traditional checkpoint mechanism that monitors the presence or function of the intact centrosome.

Materials and Methods

Cell Culture and Microsurgery:

African green monkey kidney epithelial cells (BSC-1) were obtained from ATCC (CCL-26). Cells were grown in MEM, 15mM HEPES, 10% FBS, 1% penicillin/streptomycin at 37°C under 5% CO₂ in a humidified incubator. Cells were plated onto 22mm square #1.5 coverslips in a 6-well dish. Coverslips were mounted on micromanipulation chambers as previously described (Sluder et al., 2007; Hinchcliffe et al., 2001).

Glass microneedles were made using a Kopf needle-puller (David Kopf Instruments, Tujunga, CA) and formed into a cutting implement on a micro-forge. Microsurgical removal of the centrosome was conducted using a custom X, Y, Z-axis piezo-electric micromanipulator on a modified Zeiss ACM microscope stand (Carl Zeiss Microimaging, Thornwood, NY) using a 20X phase objective. Following microsurgery, the cell was circled using a diamond scribe mounted in the objective turret. The chamber was moved to a microscope maintained at 37°C for long-term live-cell imaging. For some experiments, the coverslip was taken off of the micromanipulation chamber and re-mounted onto a sealed chamber prior to imaging.

Light Intensity Measurement:

The power output of 546nm green light at the condenser was measured at the specimen plane using a Coherent FieldMate light power meter (Coherent, Inc., Santa Clara, CA) with VIS (400-1060nm) detector head. The light intensity used for the previous study (Hinchcliffe et al., 2001a) was estimated by recreating the imaging conditions as they were recorded in lab notebooks, then measuring the light output at the condenser for the settings that provided us with equivalent quality images to those in archived data.

Live-Cell Imaging:

Cells were prepared for live-cell imaging as previously described (Sluder et al., 2007). Briefly, cells were grown on 22mm square #1.5 coverslips. Coverslips were mounted onto aluminum frame using high vacuum silicone grease (Dow Corning, Midland, MI). Cells were observed using Zeiss Universal (Carl Zeiss Microimaging, Thornwood, NY) or Olympus BH2 (Olympus America, Center Valley, PA) microscopes using 10x phase-contrast objectives. Microscopes were maintained at 37°C in cardboard boxes heated by a proportional heat control system (Omega Engineering, Stamford, CT). Images were acquired with a Hamamatsu C2400 CCD camera (Hamamatsu Photonics, Bridgewater, NJ) using Adobe Premiere 4.0 (Adobe Systems Inc., San Jose, CA) (Hinchcliffe et al., 2001; Uetake and Sluder, 2007).

Appendix B

Detailed Protocol for Observing Centrosome Duplication In a Cell-Free Extract Made From *Xenopus laevis* Oocytes

Making of *Xenopus* Oocyte Extract

The following protocol has been extensively adapted from a previously published report (Hinchcliffe and Sluder, 2001). All steps of the extract preparation were carried out at 18°C using a chilled circulating water bath. Imaging of extract experiments were also carried out at 18°C in an air-conditioned room.

Egg Collection:

Female *Xenopus laevis* frogs were housed in circulating water tanks maintained between 16-18°C. Each frog received two injections into each dorsal lymph sac the day before each experiment. At 8:00 AM, and again at 12:00 PM 250µl of 1000 IU/ml human chorionic gonadotropin (HCG) (#C1063, Sigma) was injected into each dorsal lymph sac – 500µl (500IU) each time for a total of 1ml (1000IU). Each frog was then placed, singly, into a plastic bowl with secure lid containing 1L of 1X Marc's Modified Ringers (MMR) (100mM NaCl, 2mM KCl, 1mM MgCl₂, 2mM CaCl₂, 0.1mM EGTA, 5mM HEPES (pH 7.8)). The bowls were placed into an 18°C water bath and left overnight. The following morning, the laid eggs were collected into a beaker and the frog was gently squeezed to expel any additional eggs from her body.

Frogs were kept in quarantine from the general population for at least 24 hours post egg-laying to prevent eggs from contaminating the water for the rest

of the frog colony. When eggs were no longer being expelled from the frog, she was returned to the general population.

Egg Activation:

Lain and squeezed eggs were washed 3 times using 600ml 1X MMR to remove debris. Washed eggs were rinsed 3 times with a total of 500ml 2% L-cysteine (w/v) (#C7352, Sigma) in extract buffer (XB) salts (100mM KCl, 0.1mM CaCl₂, 1mM MgCl₂) to remove jelly coats. De-jellied eggs were activated using 5µg/ml calcium ionophore A23187 (#C7522, Sigma) in 40ml of 0.2X MMR for 75 seconds. Ionophore was then washed out 7-8 times using a total of 1.5L of 0.2X MMR. Eggs were then washed 4 times with 500ml XB (XB salts with 10mM HEPES and 50mM sucrose) and once with 35ml of XB+ (XB plus protease inhibitors: Pepstatin-A (#515481, Calbiochem, EMD Biosciences, Gibbstown, NJ), Chymostatin (#C7268, Sigma), and Leupeptin (#108975, Calbiochem) each at a final concentration of 10 µg/ml). Finally, the eggs were suspended in 30ml of XB+ and ready to be transferred to a centrifuge tube.

Packing and Crushing:

Beckman Ultra-Clear centrifuge tubes (# 344057, Beckman Instruments Palo Alto, CA) were loaded with 1ml of Nyosil-M25 synthetic lubricant (Nye Lubricants Inc., Fairhaven, MA) and then layered with 1ml of XB+ containing 10µg/ml cytochalasin-D (#C8273, Sigma). The activated eggs were then gently

layered on top using a transfer pipette that had the end trimmed off. This is important so as to avoid shearing the eggs causing them to rupture. The tubes were spun in an IEC floor-stand centrifuge at 4°C at 275 x g (1,000 RPM) for 60 seconds and then the speed was increased to 620 x g (1,500 RPM) for 30 seconds. This step packed the eggs close together and displaced the buffer. All liquid (Nyosil plus buffer) was aspirated from the top of the packed eggs and the tubes were incubated at room temperature until 15 minutes had elapsed since activation. At this time the tubes were placed in a high-speed refrigerated centrifuge (Hermle) (at 4°C) and spun at 10,020 x g (8,200 RPM) for 15 minutes to crush the eggs.

Crushed eggs layered into multiple strata. The center, straw-colored layer (cytoplasm) was removed using a syringe with an 18-gauge needle pierced through the side of the centrifuge tube. The cytoplasm was slowly drawn out, transferred to a 1.5ml Eppendorf tube and placed on ice. To the extract, the three aforementioned protease inhibitors were added to a final concentration of 10µg/ml each. In addition cytochalasin-D (final concentration 10µg/ml) and Energy Mix (3.75mM creatine phosphate (#237911, Calbiochem), 0.5mM ATP (#1191, Calbiochem), 0.05mM EGTA, 0.5mM MgCl₂) were added to the extract. For S-phase arrest, Aphidicolin (#A0781, Sigma) was added to a final concentration of 5µg/ml.

Preparations for Viewing:

For all viewing chambers, 1" x 3" glass slides and 22 x 22mm #1.5 glass coverslips were bio-cleaned before use. To bio-clean glass, 2 drops of Liquinox detergent (#21837-005, VWR International, LLC, West Chester, PA) were added to 700ml of distilled water in a 1L beaker and either coverslips or slides were added. The beaker was bath sonicated at room temperature for 10 minutes. The glass was then rinsed 5x with distilled water, the beaker was refilled with deionized (18M Ω) water and bath-sonicated for another 10 minutes. The glass was then rinsed 5x with deionized water and then slides were stored in 100% ethanol. Slides and coverslips were flamed immediately prior to use using an alcohol burner to remove excess ethanol.

Chambers were constructed using a bio-cleaned slide with two layers of Teflon tape (type TV-350, CHR Industries, New Haven, CT) or Scotch Magic Tape (3M, St. Paul, MN). An 18mm square hole was cut out of the double layer of tape using a scalpel. The surface of the slide within the well, as well as the extract-facing surface of a cover slip was then thinly and evenly coated with a very small amount of silicon high vacuum grease (#14-635-5D, Fisher Scientific, Somerville, MA). This coating prevents microtubules from sticking to, and sliding across, the glass. Using a syringe, ~25 μ l of Florinert FC-43 fluorocarbon oil (3M Industrial Chemical Products Division, St. Paul, MN) was added to the well. The oil serves to prevent evaporation of the sample, and also to keep the sample contained in a well-formed pool. A 5 μ l drop of extract was then placed in the oil

and the cover slip was placed on the preparation with the silicon grease facing the sample. Any excess FC-43 was then aspirated.

Image Acquisition and Analysis

Centrosomes were visualized indirectly using polarized light microscopes: Modified Zeiss ACM stands (Carl Zeiss, Inc., Thornwood, NY) with Olympus finite tube-length optics (Olympus America, Center Valley, PA). Images were acquired using either a Hamamatsu C2400 CCD camera through an Argus20 Image processor (Hamamatsu Photonics, Bridgewater, NJ) or a Q-Imaging Retiga 1300 CCD camera via FireWire (Q-Imaging, Surrey, British Columbia, Canada). Time-lapse sequences were acquired with either Adobe Premier 6.0 (Adobe Systems Inc., San Jose, CA) or with Simple PCI 6.0 (Hamamatsu Corporation, Sewickley, PA). Final sequences were assembled using Quicktime Pro 7, utilizing PNG lossless video compression (Apple Inc., Cupertino, CA).

Quantitation of Centrosome Duplication in *Xenopus* extracts

Centrosomes were observed indirectly by following the characteristic star pattern formed by astral microtubules in polarized light microscopy. “Aster” is the term I will use to describe the organized microtubule array that represents the centrosomes. Samples were imaged every 20 seconds for 6 hours with periodic review to confirm that the centrosomes were still in focus.

Each aster was followed over time and centrosome duplication was defined as a visible doubling of an existing aster. Over the course of 6 hours, each doubling was recorded. If an aster went out of focus, or drifted out of the field of view, the entire lineage was discarded from the data set. For every aster scored, the complete lineage was known. Each aster that existed at the end of the 6-hour experiment was identified, and the number of splits that occurred from the beginning of data collection was recorded for each. See Figure 4.1.D for a diagram of how aster duplication was scored. The first doubling of the input aster happens within about 30 minutes of the start of the experiment (data not shown) and represents the separation of the pair of centrioles brought in with each sperm nucleus; followed by their duplication (Figure 4.1.D). We therefore did not count the first visible aster doubling in our analysis. Any subsequent aster doubling represents centrosome duplication. A study by Loncarek, et al. showed that the removal of a daughter centriole from the area adjacent to the mother induces the

formation of a new daughter (Loncarek et al., 2008a). That study suggests that single, unduplicated centrioles do not exist for long before a new daughter centriole is formed. A visible doubling of a microtubule aster would represent the splitting of two centrioles, followed by the immediate subsequent formation of new daughter centrioles. Therefore, we use aster doubling after the first split as an indicator of centrosome duplication.

References

- Balczon R., L. Bao, W.E. Zimmer, K. Brown, R.P. Zinkowski, and B.R. Brinkley. 1995. Dissociation of centrosome replication events from cycles of DNA synthesis and mitotic division in hydroxyurea-arrested Chinese hamster ovary cells. *Journal of Cell Biology*. 130: 105-115.
- Boveri, T. 1914. Zur Frage Der Entstehung Maligner Tumoren. Gustav Fischer, Jena, Germany. 64 pp.
- Brinkley, B.R. 2001. Managing the centrosome numbers game: from chaos to stability in cancer cell division. *Trends in Cell Biology*. 11:18-21.
- Chan, T.A., H. Hermeking, C. Lengauer, K.W. Kinzler, and B. Vogelstein. 1999. 14-3-3Sigma is required to prevent mitotic catastrophe after DNA damage. *Nature*. 401:616-620.
- Chiba, S., M. Okuda, J.G. Mussman, and K. Fukasawa. 2000. Genomic convergence and suppression of centrosome hyperamplification in primary p53^{-/-} cells in prolonged culture. *Experimental Cell Research*. 258:310-321.
- Cimini, D., B. Howell, P. Maddox, A. Khodjakov, F. Degrossi, and E.D. Salmon. 2001. Merotelic kinetochore orientation is a major mechanism of aneuploidy in mitotic mammalian tissue cells. *Journal of Cell Biology*. 153:517-527.
- Compton, D.A. 2000. Spindle assembly in animal cells. *Annual Review of Biochemistry*. 69:95-114.
- Dammerman, A., P. Maddox, A. Desai, and K. Oegema. 2008. SAS-4 is recruited to a dynamic structure in newly forming centrioles that is stabilized by the gamma-tubulin-mediated addition of centriolar microtubules. *Journal of Cell Biology*. 180:771-785.
- D'assoro, A., W.L. Lingle, and J.L. Salisbury. 2002. Centrosome amplification and the development of cancer. *Oncogene*. 21:6146-6153.
- Delaval, B., and S.J. Doxsey. 2010. Pericentrin in cellular function and disease. *Journal of Cell Biology*. 188:181-190.
- Doxsey, S. 2001a. Re-evaluating centrosome function. *Nature Reviews Molecular Cell Biology*. 2:688-698.
- Doxsey, S.J. 2001b. Centrosomes as command centres for cellular control. *Nature Cell Biology*. 3:E105-108.

- Duensing, S., and K. Münger. 2002. Human papillomaviruses and centrosome duplication errors: modeling the origins of genomic instability. *Oncogene*. 21:6241-6248.
- Eckerdt, F., T.M. Yamamoto, A.L. Lewellyn, and J.L. Maller. 2011. Identification of a Polo-like Kinase 4-Dependent Pathway for De Novo Centriole Formation. *Current Biology*. 21:428-432.
- Evans, L., T. Mitchison, M. Kirschner. 1985. Influence of the centrosome on the structure of nucleated microtubules. *Journal of Cell Biology*. 100: 1185-1191.
- Fellers, T.J., M.W. Davidson, and The Florida State University. 2005. Molecular Expressions Microscopy Primer: Digital Imaging in Optical Microscopy - Concepts in Digital Imaging - CCD Saturation and Blooming.
- Ferguson, R.L., and J.L. Maller. 2010. Centrosomal localization of cyclin E-Cdk2 is required for initiation of DNA synthesis. *Current Biology*. 20:856-860.
- Ferguson, R.L., and J.L. Maller. 2008. Cyclin E-dependent localization of MCM5 regulates centrosome duplication. *Journal of Cell Science*. 121:3224-3232.
- Ferguson, R.L., G. Pascreau, and J.L. Maller. 2010. The cyclin A centrosomal localization sequence recruits MCM5 and Orc1 to regulate centrosome reduplication. *Journal of Cell Science*. 123:2743-2749.
- Freed, E., K.R. Lacey, P. Huie, S.A. Lyapina, R.J. Deshaies, T. Stearns, and P.K. Jackson. 1999. Components of an SCF ubiquitin ligase localize to the centrosome and regulate the centrosome duplication cycle. *Genes & Development*. 13:2242-2257.
- Fukasawa, K. 2007. Oncogenes and tumour suppressors take on centrosomes. *Nature Reviews Cancer*. 7:911-924.
- Fukasawa, K., T. Choi, R. Kuriyama, S. Rulong, and G. Vande Woude. 1996. Abnormal centrosome amplification in the absence of p53. *Science*. 271:1744-1747.
- Fukasawa, K., F. Wiener, G. Vande Woude, and S. Mai. 1997. Genomic instability and apoptosis are frequent in p53 deficient young mice. *Oncogene*. 15:1295-1302.
- Galipeau, P.C., D.S. Cowan, C.A. Sanchez, M.T. Barrett, M.J. Emond, D.S. Levine, P.S. Rabinovitch, and B.J. Reid. 1996. 17p (p53) allelic losses, 4N

(G2/tetraploid) populations, and progression to aneuploidy in Barrett's esophagus. *Proceedings of the National Academy of Sciences of the United States of America*. 93:7081-7084.

Ganem, N.J., S.A. Godinho, and D. Pellman. 2009. A mechanism linking extra centrosomes to chromosomal instability. *Nature*. 460:278-282.

Goepfert, T.M., Y.E. Adigun, L. Zhong, J. Gay, D. Medina, and W.R. Brinkley. 2002. Centrosome amplification and overexpression of aurora A are early events in rat mammary carcinogenesis. *Cancer Research*. 62:4115-4122.

Hartley, R.S., R.E. Rempel, and J.L. Maller. 1996. In vivo regulation of the early embryonic cell cycle in *Xenopus*. *Developmental Biology*. 173:408-419.

Heald, R., R. Tournebize, A. Habermann, E. Karsenti, and A. Hyman. 1997. Spindle assembly in *Xenopus* egg extracts: respective roles of centrosomes and microtubule self-organization. *Journal of Cell Biology*. 138:615-628.

Heneen, W.K. 1975. Kinetochores and microtubules in multipolar mitosis and chromosome orientation. *Experimental Cell Research*. 91:57-62.

Heneen, W.K. 1970. In situ analysis of normal and abnormal patterns of the mitotic apparatus in cultured rat-kangaroo cells. *Chromosoma*. 29:88-117.

Hinchcliffe, E. 2001. "It Takes Two to Tango": understanding how centrosome duplication is regulated throughout the cell cycle. *Genes & Development*. 15:1167-1181.

Hinchcliffe, E.H., G.O. Cassels, C.L. Rieder, and G. Sluder. 1998. The coordination of centrosome reproduction with nuclear events of the cell cycle in the sea urchin zygote. *Journal of Cell Biology*. 140:1417-1426.

Hinchcliffe, E.H., C. Li, E.A. Thompson, J.L. Maller, and G. Sluder. 1999. Requirement of Cdk2-cyclin E activity for repeated centrosome reproduction in *Xenopus* egg extracts. *Science*. 283:851-854.

Hinchcliffe, E.H., F. Miller, M. Cham, A. Khodjakov, and G. Sluder. 2001. Requirement of a Centrosomal Activity for Cell Cycle Progression Through G1 into S Phase. *Science*. 291:1547-1550.

Hinchcliffe, E.H., and G. Sluder. 2002. Two for two: Cdk2 and its role in centrosome doubling. *Oncogene*. 21:6154-6160.

Hinchcliffe, E.H., and G. Sluder. 2001. Centrosome reproduction in *Xenopus* lysates. *Methods in Cell Biology*. 67:269-287.

Hinchcliffe, E.H., and G. Sluder. 1998. "Do Not (Mis-)Adjust Your Set": Maintaining Specimen Detail in the Video Microscope. *Methods in Cell Biology*. 72:65-85.

Hornick, J.E., C.C. Mader, E.K. Tribble, C.C. Bagne, K.T. Vaughan, S.L. Shaw, and E.H. Hinchcliffe. 2011. Amphiatral mitotic spindle assembly in vertebrate cells lacking centrosomes. *Current Biology*. 21:598-605.

Karsenti, E., and I. Vernos. 2001. The mitotic spindle: a self-made machine. *Science*. 294:543-547.

Khodjakov, A., R.W. Cole, B.R. Oakley, and C.L. Rieder. 2000. Centrosome-independent mitotic spindle formation in vertebrates. *Current Biology*. 10:59-67.

Khodjakov, A., and C.L. Rieder. 2001. Centrosomes enhance the fidelity of cytokinesis in vertebrates and are required for cell cycle progression. *Journal of Cell Biology*. 153:237-242.

Kleylein-Sohn, J., J. Westendorf, M. Le Clech, R. Habedanck, Y.D. Stierhof, and E.A. Nigg. 2007. Plk4-induced centriole biogenesis in human cells. *Developmental Cell*. 13:190-202.

Krämer, A., K. Neben, and A.D. Ho. 2002. Centrosome replication, genomic instability and cancer. *Leukemia*. 16:767-775.

Krude, T., M. Jackman, J. Pines, and R.A. Laskey. 1997. Cyclin/Cdk-dependent initiation of DNA replication in a human cell-free system. *Cell*. 88:109-119.

Kwon, M., S.A. Godinho, N.S. Chandhok, N.J. Ganem, A. Azioune, M. They, and D. Pellman. 2008. Mechanisms to suppress multipolar divisions in cancer cells with extra centrosomes. *Genes and Development*. 22:2189-2203.

Lacey, K.R., P.K. Jackson, and T. Stearns. 1999. Cyclin-dependent kinase control of centrosome duplication. *Proceedings of the National Academy of Sciences of the United States of America*. 96:2817-2822.

Lengauer, C., K.W. Kinzler, and B. Vogelstein. 1998. Genetic instabilities in human cancers. *Nature*. 396:643-649.

Levesque, A.A., L. Howard, M.B. Gordon, and D.A. Compton. 2003. A functional relationship between NuMA and kid is involved in both spindle organization and

chromosome alignment in vertebrate cells. *Molecular Biology of the Cell*. 14:3541-3552.

Levine, D.S., C.A. Sanchez, P.S. Rabinovitch, and B.J. Reid. 1991. Formation of the tetraploid intermediate is associated with the development of cells with more than four centrioles in the elastase-simian virus 40 tumor antigen transgenic mouse model of pancreatic cancer. *Proceedings of the National Academy of Sciences of the United States of America*. 88:6427-6431.

Lingle, W.L., S.L. Barrett, V.C. Negron, A. D'assoro, K. Boeneman, W. Liu, C.M. Whitehead, C. Reynolds, and J.L. Salisbury. 2002. Centrosome amplification drives chromosomal instability in breast tumor development. *Proceedings of the National Academy of Sciences of the United States of America*. 99:1978-1983.

Lingle, W.L., W.H. Lutz, J.N. Ingle, N.J. Maihle, and J.L. Salisbury. 1998. Centrosome hypertrophy in human breast tumors: implications for genomic stability and cell polarity. *Proceedings of the National Academy of Sciences of the United States of America*. 95:2950-2955.

Lingle, W.L., and J.L. Salisbury. 2000. The role of the centrosome in the development of malignant tumors. *Current Topics in Developmental Biology*. 49:313-329.

Lingle, W.L., and J.L. Salisbury. 1999. Altered centrosome structure is associated with abnormal mitoses in human breast tumors. *The American Journal of Pathology*. 155:1941-1951.

Loncarek, J., P. Hergert, V. Magidson, and A. Khodjakov. 2008. Control of daughter centriole formation by the pericentriolar material. *Nature Cell Biology*. 10:322-328.

Matsumoto, Y., K. Hayashi, and E. Nishida. 1999. Cyclin-dependent kinase 2 (Cdk2) is required for centrosome duplication in mammalian cells. *Current Biology*. 9:429-432.

Matsumoto, Y., and J.L. Maller. 2004. A centrosomal localization signal in cyclin E required for Cdk2-independent S phase entry. *Science*. 306:885-888.

Mazia, D. 1984. Centrosomes and mitotic poles. *Experimental Cell Research*. 153:1-15.

Meads, T., and T.A. Schroer. 1995. Polarity and nucleation of microtubules in polarized epithelial cells. *Cell Motility and the Cytoskeleton*. 32:273-288.

- Mikule, K., B. Delaval, P. Kaldis, A. Jurczyk, P. Hergert, and S. Doxsey. 2007. Loss of centrosome integrity induces p38-p53-p21-dependent G1-S arrest. *Nature Cell Biology*. 9:160-170.
- Musch, A. 2004. Microtubule organization and function in epithelial cells. *Traffic*. 5:1-9.
- Nigg, E.A. 2002. Centrosome aberrations: cause or consequence of cancer progression? *Nature Reviews Cancer*. 2:815-825.
- O'Connell, K.F., C. Caron, K.R. Kopish, D.D. Hurd, K.J. Kemphues, Y. Li, and J.G. White. 2001. The *C. elegans* zyg-1 gene encodes a regulator of centrosome duplication with distinct maternal and paternal roles in the embryo. *Cell*. 105:547-558.
- Ohtsubo, M., A.M. Theodoras, J. Schumacher, J.M. Roberts, and M. Pagano. 1995. Human cyclin E, a nuclear protein essential for the G1-to-S phase transition. *Molecular and Cellular Biology*. 15:2612-2624.
- Orr-Weaver, T., and R.A. Weinberg. 1998. A checkpoint on the road to cancer. *Nature*. 392:223-224.
- Pascreau, G., M.E. Churchill, and J.L. Maller. 2011. Centrosomal localization of cyclins E and A: structural similarities and functional differences. *Cell Cycle*. 10:199-205.
- Piel, M., J. Nordberg, U. Euteneuer, and M. Bornens. 2001. Centrosome-Dependent Exit of Cytokinesis in Animal Cells. *Science*. 291:1550-1553.
- Pihan, G.A., A. Purohit, J. Wallace, H. Knecht, B. Woda, P. Quesenberry, and S.J. Doxsey. 1998. Centrosome defects and genetic instability in malignant tumors. *Cancer Research*. 58:3974-3985.
- Pihan, G.A., A. Purohit, J. Wallace, R. Malhotra, L. Liotta, and S.J. Doxsey. 2001. Centrosome defects can account for cellular and genetic changes that characterize prostate cancer progression. *Cancer Research*. 61:2212-2219.
- Pihan, G.A., J. Wallace, Y. Zhou, and S.J. Doxsey. 2003. Centrosome abnormalities and chromosome instability occur together in pre-invasive carcinomas. *Cancer Research*. 63:1398-1404.
- Quintyne, N.J., J.E. Reing, D.R. Hoffelder, S.M. Gollin, and W.S. Saunders. 2005. Spindle multipolarity is prevented by centrosomal clustering. *Science*. 307:127-129.

Rempel, R.E., S.B. Sleight, and J.L. Maller. 1995. Maternal *Xenopus* Cdk2-cyclin E complexes function during meiotic and early embryonic cell cycles that lack a G1 phase. *Journal of Biological Chemistry*. 270:6843-6855.

Ried, T., K. Heselmeyer-Haddad, H. Blegen, E. Schröck, and G. Auer. 1999. Genomic changes defining the genesis, progression, and malignancy potential in solid human tumors: a phenotype/genotype correlation. *Genes Chromosomes Cancer*. 25:195-204.

Rieder, C.L., and G.G. Borisy. 1982. The Centrosome Cycle in PtK2 Cells - Asymmetric Distribution and Structural Changes in the Pericentriolar Material. *Biology of the Cell*. 44:117-132.

Rieder, C.L., S. Faruki, and A. Khodjakov. 2001. The centrosome in vertebrates: more than a microtubule-organizing center. *Trends in Cell Biology*. 11:413-419.

Rieder, C.L., and E.D. Salmon. 1998. The vertebrate cell kinetochore and its roles during mitosis. *Trends in Cell Biology*. 8:310-318.

Ring, D., R. Hubble, and M. Kirschner. 1982. Mitosis in a cell with multiple centrioles. *Journal of Cell Biology*. 94:549-556.

Rodrigues-Martins, A., M. Bettencourt-Dias, M. Riparbelli, C. Ferreira, I. Ferreira, G. Callaini, and D.M. Glover. 2007. DSAS-6 organizes a tube-like centriole precursor, and its absence suggests modularity in centriole assembly. *Current Biology*. 17:1465-1472.

Roper Scientific. 2006. Gain - Photometrics Imaging Learning Zone.

Rosenblatt, J., Y. Gu, and D.O. Morgan. 1992. Human cyclin-dependent kinase 2 is activated during the S and G2 phases of the cell cycle and associates with cyclin A. *Proceedings of the National Academy of Sciences of the United States of America*. 89:2824-2828.

Sato, N., K. Mizumoto, M. Nakamura, K. Nakamura, M. Kusumoto, H. Niiyama, T. Ogawa, and M. Tanaka. 1999. Centrosome abnormalities in pancreatic ductal carcinoma. *Clinical Cancer Research*. 5:963-970.

Savoian, M.S., W.C. Earnshaw, A. Khodjakov, and C.L. Rieder. 1999. Cleavage furrows formed between centrosomes lacking an intervening spindle and chromosomes contain microtubule bundles, INCENP, and CHO1 but not CENP-E. *Molecular Biology of the Cell*. 10:297-311.

- Schnackenberg, B., W. Marzluff, and G. Sluder. 2008. Cyclin E in centrosome duplication and reduplication in sea urchin zygotes. *Journal of Cellular Physiology*. 217:626-631.
- Schnackenberg, B.J., and R.E. Palazzo. 1999. Identification and function of the centrosome centromatrix. *Biology of the Cell*. 91:429-438.
- Scholey, J.M., I. Brust-Mascher, and A. Mogilner. 2003. Cell division. *Nature*. 422:746-752.
- Shackney, S.E., C.A. Smith, B.W. Miller, D.R. Burholt, K. Murtha, H.R. Giles, D.M. Ketterer, and A.A. Pollice. 1989. Model for the genetic evolution of human solid tumors. *Cancer Research*. 49:3344-3354.
- Shi, Q., and R.W. King. 2005. Chromosome nondisjunction yields tetraploid rather than aneuploid cells in human cell lines. *Nature*. 437:1038-1042.
- Shono, M., N. Sato, K. Mizumoto, N. Maehara, M. Nakamura, E. Nagai, and M. Tanaka. 2001. Stepwise progression of centrosome defects associated with local tumor growth and metastatic process of human pancreatic carcinoma cells transplanted orthotopically into nude mice. *Laboratory Investigation*. 81:945-952.
- Sillibourne, J.E., F. Tack, N. Vloemans, A. Boeckx, S. Thambirajah, P. Bonnet, F.C. Ramaekers, M. Bornens, and T. Grand-Perret. 2010. Autophosphorylation of polo-like kinase 4 and its role in centriole duplication. *Molecular Biology of the Cell*. 21:547-561.
- Skyldberg, B., K. Fujioka, A. Hellström, L. Sylvén, B. Moberger, and G. Auer. 2001. Human papillomavirus infection, centrosome aberration, and genetic stability in cervical lesions. *Modern Pathology*. 14:279-284.
- Sluder, G., F.J. Miller, and C.L. Rieder. 1986. The reproduction of centrosomes: nuclear versus cytoplasmic controls. *Journal of Cell Biology*. 103:1873-1881.
- Sluder, G., and J.J. Nordberg. 2004. The good, the bad and the ugly: the practical consequences of centrosome amplification. *Current Opinion in Cell Biology*. 16:49-54.
- Sluder, G., J.J. Nordberg, F.J. Miller, and E.H. Hinchcliffe. 2007. A sealed preparation for long-term observations of cultured cells. *CSH Protoc*. 2007:pdb.prot4660.
- Sluder, G., E.A. Thompson, F.J. Miller, J. Hayes, and C.L. Rieder. 1997. The checkpoint control for anaphase onset does not monitor excess numbers of

spindle poles or bipolar spindle symmetry. *Journal of Cell Science*. 110 (Pt 4):421-429.

Sluder, G. 1992. Control of centrosome inheritance in echinoderm development. In *The Centrosome*. V. Kalnin editor. Academic Press/San Diego. 235-239.

Sluder, G. 2004. Centrosome Duplication and its Regulation in the Higher Animal Cell. In *Centrosomes in Development and Disease*. E. Nigg editor. Wiley VCH/Weinheim. 167-189.

Solecki, D.J., L. Model, J. Gaetz, T.M. Kapoor, and M.E. Hatten. 2004. Par6alpha signaling controls glial-guided neuronal migration. *Nature Neuroscience*. 7:1195-1203.

Southern, S.A., M.F. Evans, and C.S. Herrington. 1997. Basal cell tetrasomy in low-grade cervical squamous intraepithelial lesions infected with high-risk human papillomaviruses. *Cancer Research*. 57:4210-4213.

Sumerel, J.L., J.C. Moore, B.J. Schnackenberg, J.A. Nichols, J.C. Canman, G.M. Wessel, and W.F. Marzluff. 2001. Cyclin E and its associated cdk activity do not cycle during early embryogenesis of the sea Urchin. *Developmental Biology*. 234:425-440.

Takisawa, H., S. Mimura, and Y. Kubota. 2000. Eukaryotic DNA replication: from pre-replication complex to initiation complex. *Current Opinion in Cell Biology*. 12:690-696.

Tarapore, P., and K. Fukasawa. 2002. Loss of p53 and centrosome hyperamplification. *Oncogene*. 21:6234-6240.

Tsou, M.F., and T. Stearns. 2006. Mechanism limiting centrosome duplication to once per cell cycle. *Nature*. 442:947-951.

Uetake, Y., J. Loncarek, J. Nordberg, C. English, S. La Terra, A. Khodjakov, and G. Sluder. 2007. Cell cycle progression and de novo centriole assembly after centrosomal removal in untransformed human cells. *The Journal of Cell Biology*. 176:173-182.

Uetake, Y., and G. Sluder. 2007. Cell-cycle progression without an intact microtubule cytoskeleton. *Current Biology*. 17:2081-2086.

van der Huevel, S., and E. Harlow. 1993. Distinct Roles for Cyclin-Dependent Kinases in Cell Cycle Control. *Science*. 262:2050-2054.

Wong, C., and T. Stearns. 2003. Centrosome number is controlled by a centrosome-intrinsic block to reduplication. *Nature Cell Biology*. 5:539-544.